Saudi Pharmaceutical Journal 31 (2023) 101727

HOSTED BY

Contents lists available at ScienceDirect

Saudi Pharmaceutical Journal

journal homepage: www.sciencedirect.com

Original article

Statistical optimization of tetrahydrocurcumin loaded solid lipid nanoparticles using Box Behnken design in the management of streptozotocin-induced diabetes mellitus

Jai Bharti Sharma [a], Shailendra Bhatt [b,*], Abhishek Tiwari [c], Varsha Tiwari [c], Manish Kumar [d,*], Ravinder Verma [e], Deepak Kaushik [f], Tarun Virmani [g], Girish Kumar [g], Omkulthom Al kamaly [h], Asmaa Saleh [h], Mohammed Khalid Parvez [i], Abdulsalam Alhalmi [j]

[a] M.M. College of Pharmacy, Maharishi Markandeshwar (Deemed to be) University, Mullana, Haryana, India
[b] Shrinathji Institute of Pharmacy, Shrinathji Society for Higher Education Upali Oden, Nathdwara, Rajasmand, Rajasthan, India
[c] Pharmacy Academy, IFTM University, Lodhipur-Rajput, Moradabad 244102, U.P., India
[d] School of Pharmaceutical Sciences, CT University, Ludhiana, Punjab, India
[e] Department of Pharmaceutical Sciences, Chaudhary Bansi Lal, University, Bhiwani 127021, India
[f] Department of Pharmaceutical Sciences, M.D. University, Rohtak, Haryana, India
[g] School of Pharmaceutical Sciences, MVN University, Palwal, Haryana 121105, India
[h] Department of Pharmaceutical Sciences, College of Pharmacy, Princess Nourah bint Abdulrahman University, P.O Box 84428, Riyadh 11671, Saudi Arabia
[i] Department of Pharmacognosy, College of Pharmacy, King Saud University, Riyadh 11451, Saudi Arabia
[j] Department of Pharmaceutics School of Pharmaceutical Education and Research, Jamia Hamdard, New Delhi 110062, India

ARTICLE INFO

Article history:
Received 10 May 2023
Accepted 27 July 2023
Available online 2 August 2023

Keywords:
Tetrahydrocurcumin
Box-Behnken design
SLN
Pharmacokinetic study
Pharmacodynamic study
STZ-induced Diabetes Mellitus

ABSTRACT

In the past, curcumin was the go-to medication for diabetes, but recent studies have shown that tetrahydrocurcumin is more effective. The problem is that it's not very soluble in water or very bioavailable. So, our research aims to increase the bioavailability and anti-diabetic efficacy of tetrahydrocurcumin in streptozotocin-induced diabetic rats by synthesizing tetrahydrocurcumin-loaded solid lipid nanoparticles. Box Behnken Design was employed for the optimization of tetrahydrocurcumin-loaded solid lipid nanoparticles (THC-SLNs). The optimal formulation was determined by doing an ANOVA to examine the relationship between the independent variables (drug-to-lipid ratio, surfactant concentration, and co-surfactant concentration) and the dependent variables (particle size, percent entrapment efficiency, and PDI). Particle size, PDI, and entrapment efficiency all showed statistical significance based on F-values and p-values. The optimized batch was prepared using a drug-to-lipid ratio (1:4.16), 1.21% concentration of surfactant, and 0.4775% co-surfactant (observed with a particle size of 147.1 nm, 83.58 ± 0 .838 % entrapment efficiency, and 0.265 PDI, and the values were found very close with the predicted ones. As the THC peak vanishes from the DSC thermogram of the improved formulation, this indicates that the drug has been transformed from its crystalline form into its amorphous state. TEM analysis of optimized formulation demonstrated mono-dispersed particles with an average particle size of 145 nm which are closely related to zetasizer's results. In-vitro release study of optimized formulation demonstrated burst release followed by sustained release up to 71.04% throughout 24 hrs. Increased bioavailability of the adjusted THC-SLN was found in an in vivo pharmacokinetics research with 9.47 folds higher $AUC_{(0-t)}$ compared to plain THC-suspension. Additionally, pharmacodynamic experiments of optimized formulation demonstrated a marked decrease in blood glucose level to 63.7% and increased body

* Corresponding authors.
E-mail addresses: bhartikaushish@gmail.com (J. Bharti Sharma), shailu.bhatt@gmail.com (S. Bhatt), abhishekt1983@gmail.com (A. Tiwari), varshat1983@gmail.com (V. Tiwari), manish_singh17@rediffmail.com (M. Kumar), ravinderbasniwal7661@gmail.com (R. Verma), deepkaushik@rediffmail.com (D. Kaushik), tarun.virmani@mvn.edu.in (T. Virmani), girish.kumar@mvn.edu.in (G. Kumar), omalkmali@pnu.edu.sa (O. Al kamaly), asali@pnu.edu.sa (A. Saleh), mohkhalid@ksu.edu.sa (M. Khalid Parvez), asalamahmed5@gmail.com (A. Alhalmi).

Peer review under responsibility of King Saud University.

Production and hosting by Elsevier

https://doi.org/10.1016/j.jsps.2023.101727

weight from 195.8 ± 7.223 to 231.2 ± 7.653 on the 28th day of the study and showed a better anti-diabetic effect than plain drug suspension. Results of stability studies revealed that formulation can be stored for longer periods at room temperature. Tetrahydrocurcumin can be effectively administered by SLN for the treatment of diabetes.

1. Introduction

Curcumin is a polyphenolic compound used in the treatment of various diseases. It is obtained from turmeric which is mentioned in Ayurveda as a medicinal plant of curcuma species (Farsani et al., 2021; Kumar et al., 2023). Tetrahydrocurcumin (THC) possesses the same pharmacological properties as curcumin as it is a major metabolite of curcumin. It is more stable in the intestine and 0.1 M phosphate buffers of various Ph. It has more antioxidant potential compared to curcumin while the pro-oxidant and anti-inflammatory activities are higher in curcumin (Trivedi et al., 2020). Diabetes mellitus characterized by hyperglycemia and metabolic alternation is carbohydrates, lipid and proteins is considered worldwide as a most challenging chronic disease (El-Bagory et al., 2019). Diabetes mellitus can be prevented or treated using plant products and among these curcumin can be used in various aspects like insulin resistance, increasing lipid level, increased blood glucose level, necrosis, and β-cell dysfunction (Zhang et al., 2013). THC shows more effectiveness in the treatment of diabetes mellitus and hyperlipidemia compared to curcumin as it enhances the plasma insulin level and reduces the blood glucose, liver cholesterol, triglycerides, and phospholipid level (Yuan et al., 2020). Several effects of THC i.e. antihyperlipidemic (Pari and Murugan, 2007), antioxidant (Murugan and Pari, 2006a), on blood glucose and plasma insulin (Pari and Murugan, 2005), on plasma antioxidants (Murugan and Pari, 2006b), lipid peroxidation (Murugan and Pari, 2006c), protein level, and hepatic & renal functional markers are reported in streptozotocin-induced diabetic rats by Pari and Murugan (Murugan and Pari, 2007). They reported higher effectiveness of THC than compared to curcumin in every aspect of diabetes mellitus. But it has poor efficacy, due to incomplete release at the site of absorption, short gastric emptying time, poor aqueous solubility, and primary excretion via the non-renal route (Lai et al., 2020; Setthacheewakul et al., 2011). In a study, the in vitro release of THC was found to be 94.24% from the electrospun nanofibers and its transdermal diffusivity confirms its suitability for wound healing or other skin ailments (Rramaswamy et al., 2018). Solid lipid nanoparticles (SLNs) with 10–1000 nm particle size are spherical in shape and have multiple advantages over the other nanoformulations (Kumar et al., 2022a). These contain solid lipids and surfactants and can be easily prepared on a lab-scale (Rana et al., 2020). They are effective for the delivery of active ingredients *via* oral, skin, nasal, or any other route as they are biologically safe and can be stored for longer periods (Ganesan et al., 2018; Virmani et al., 2022). These are suitable for hydrophilic as well as hydrophobic drugs with high resistance power in gastric environment (Shaveta et al., 2020). SLN prevent the gastrointestinal degradation of drug and increase lymphatic uptake of drugs thus enhancing the bioavailability of the drugs (Alhalmi et al., 2022c; S. Bhatt et al., 2018). Kakkar et al. developed the SLN of THC and efficiently delivered them topically in skin inflammation (Kakkar et al., 2018). As per literature search, no nanoformulation is available for the delivery of THC orally which overcomes its limitations like poor aqueous solubility. In a study, the aqueous solubility and bioavailability of the THC were enhanced by a self-micro emulsifying drug delivery system (Sermkaew et al., 2013).

SLNs were developed in our study for the oral administration of THC for diabetes mellitus management in streptozotocin-induced diabetic rats. The effect of selected independent variables (drug-to-lipid ratio, surfactant concentration, and co-surfactant concentration) and their interaction were checked on the dependent variables (particle size, percent entrapment efficiency, and PDI). Statistical analysis of experimental data was done using ANOVA.

2. Materials and methods

2.1. Chemicals

Tetrahydrocurcumin was provided as a free sample by Sunpure Extracts Pvt. Ltd., India. Streptozotocin was procured from Sigma Aldrich (Germany). Sodium lauryl sulfate and glyceryl monostearate (GMS) were procured from Central Drug House (P) Ltd., New Delhi. Tween 80 was purchased from Qualikems Fine Chem. The rest of the chemicals used were of analytical grade and were obtained from the MM College of Pharmacy, Mullana, Ambala, India.

2.2. Instruments

After in vitro drug release, samples were analyzed using a double-beam UV–visible spectrophotometer (Shimadzu, UV-1800). The thermal analysis of the pure drug and the formulation were conducted using a DSC Q20 V24.11 Build 124 and a Perkin Elmer- DSC-8000, respectively. Zetasizer was used to measure the particle size, zeta potential, and polydispersity index (PDI) (Malvern Zetasizer, Ver. 7.11). The transmission electron microscope was used to examine the morphology of the improved SLN (H-7500, Hitachi Ltd., Japan). In vitro, experiments were performed using a dialysis membrane (molecular weight cut off: 12–14 kDa) from Himedia, Mumbai, India. A Spectrum FT-IR/FIR Spectrometer-400 from Perkin Elmer, USA, was used to perform the FTIR (Fourier Transform InfraRed) analysis.

2.3. Preliminary screening

2.3.1. Selection of lipid

Solubility studies were used for the selection of lipids. 500 mg of each lipid was melted at a temperature not exceeding 5 °C of their melting point on the water bath. THC was added in increments of 5 mg till a clear solution was obtained. The quantity of drug added before the precipitation observed was considered as the solubility of the drug (Hazzah et al., 2015).

2.3.2. Selection of surfactant and co-surfactant

It is reported in the literature that a surfactant of optimum HLB is required for the stabilization of the SLN formulation. Tween 80 with an HLB value of 15, produces stable SLN with optimum particle size (Gaur et al., 2014). In a study, a formulation containing tween 80 was observed with small particle size as compared to Tego care, the results were correlated with the HLB value of Tween 80 (Sznitowska et al., 2017). So, we have selected tween 80 as a surfactant. We have selected soy lecithin as a co-surfactant as it

provides the film strength to SLN so that the maximum drug can be entrapped in the lipid (Tan et al., 2017).

2.3.3. Selection of drug, lipid, and surfactant concentration

As per the literature review, the maximum concentration for the drug-to-lipid ratio, surfactant, and co-surfactant used for the trial batches are 1:10, 3%, and 1%. For the selection of the best combination of excipients, the prepared SLNs were visually observed for gelation, phase separation, and creamy effect.

2.4. Preparation of THC-loaded SLN using experimental design

2.4.1. Preparation of THC-loaded SLN (THC-SLN)

SLN were prepared by the previously published method of Ban et al., 2020; with slight modification in which emulsification followed by sonication was employed (Ban et al., 2020). Glyceryl monostearate, soy lecithin, and THC were used in the lipid phase and tween 80 in the aqueous phase. Both phases were heated separately at 70 °C. After heating, a high-speed mechanical stirrer was used for mixing the aqueous phase in the lipid phase and temperature was maintained at 70 °C. The stirring rate was maintained for 30 min at 70 °C. Sonication was performed for 8 min at 40% amplitude using a probe sonicator to reduce the globule size as the globules can be breakdown using maximum energy for a long time at high temperatures (Sharma et al., 2021). But beyond a limit, the increasing amplitude and time cause particle aggregation thus increasing the particle size (Behbahani et al., 2017). After sonication, the prepared SLNs were immediately stored at 4 °C.

2.4.2. Selection of formulation variables

Three levels (+1,0 and −1) of the drug-to-lipid ratio, concentration of surfactant, and co-surfactant concentration (independent variables) were selected as shown in Table 1.

2.4.3. Experimental design

Box Behnken Design was used to conduct all the experiments as it consumes less time with less runs (Yasir et al., 2021; 2018). The design was implemented using a trial version of Design Expert® software that suggested a total of 15 experimental runs with three center points to minimize the uncontrolled variables as shown in Table 2. These suggested formulations were developed and analyzed for selected responses.

2.5. Statistical analysis

Study of variance (ANOVA) was used in conjunction with Design Expert® software to conduct the statistical analysis of variables. There was an examination of the formulation variables and their interaction to see how they affected the outcomes. Using sequential p-value, lack of fit p-value, adjusted R^2, and forecasted R^2, the Design Expert® software determined the best-fitting model. P-values<0.05 and F-values greater than 0.05 indicate that each component has a significant contribution (Behbahani et al., 2017). The connection between causes and effects can be visualized using counter and 3-D surface graphs (Dudhipala and Janga, 2017). In a polynomial equation, a diminishing effect on the response is represented by a negative sign for the magnitude of the coefficient and an increasing effect by a positive sign (Alhalmi et al., 2022a).

2.6. Selection of optimized formulation

To get the best possible particle size, PDI, and entrapment efficiency, the THC-SLN was optimized. Optimization was performed using a numerical approach based on a desired function ranging from 0 to 1 and an overlay plot derived from a graphical method. The optimal formulation was created using the predicted values of the variables with the highest desire function. The results of the predictions were compared to the actual results (Syed et al., 2021).

2.7. Determining the nature of SLN

2.7.1. Particle size and PDI

After diluting the newly produced SLNs formulations with distilled water 100 times, particle size and PDI were measured using a Malvern zetasizer (Malvern, UK). It was done three times to ensure accuracy.

2.7.2. Percent entrapment efficiency

1 ml of prepared formulations was centrifuged for 45 min at 18000 rpm and 4℃ using a cooling centrifuge separately (Priyanka et al., 2018). The UV–Visible spectrophotometer was used for the determination of the unentrapped drug by analyzing the supernatant. The percent entrapment efficiency (%EE) was calculated using **Equation (1)** as given below:

$$\%\,\mathrm{EE} = \frac{\text{Total drug added} - \text{Unentrapped drug}}{\text{Total drug added}} X100 \quad (1)$$

2.8. Optimized formulation characterization

2.8.1. Particle size, zeta potential, and PDI

The optimized formulation was analyzed for determination of particle size, zeta potential, and PDI in triplicate after diluted 100 times with distilled water using Malvern zetasizer (Malvern, UK).

2.8.2. Drug content

The concentration of the drug was ascertained by sonicating 0.1 ml of SLN for 2 min in 10 ml of methanol and then filtering the mixture through a 0.45-μm syringe filter (Padhye and Nagarsenker, 2013). The potency of the drugs was determined by spectrophotometric analysis at 280 nm using the following equation:

$$\text{Drug content} = \frac{\text{Amount of drug obtained}}{\text{Total amount of drug}} X100 \quad (2)$$

2.8.3. In-vitro release study

The solubility studies of THC were conducted in simulated gastric fluid pH 1.2, simulated intestinal fluid (SIF) pH 6.8, and SIF 7.4. THC was discovered to be more soluble in simulated intestinal fluid

Table 1
Components used in Box Behnken Design.

Factor	Name	Units	Level		
			High (+1)	Medium (0)	Low (-1)
A	Drug-to-lipid ratio		1:6	1:4.5	1:3
B	Surfactant concentration	%	2.50	1.75	1
C	Co-surfactant concentration	%	0.20	0.35	0.5

Table 2
Values obtained after several experimental runs were conducted using Box Behnken Design.

Run	Drug-to-lipid ratio	Surfactant concentration (%)	Co-surfactant concentration (%)	Particle Size (nm)	EE (%)	PDI	Zeta Potential (mV)
1	1:3	1.75	0.50	125.4	69.1 ± 1.27	0.125	−21.0
2	1:4.5	1	0.50	184	85.3 ± 0.98	0.291	−25.7
3	1:4.5	2.5	0.20	131.7	79.3 ± 1.24	0.239	−20.3
4	1:4.5	1.75	0.35	149.3	84.1 ± 0.93	0.287	−23.1
5	1:4.5	2.5	0.50	127	82.7 ± 0.96	0.206	−19.9
6	1:6	2.5	0.35	317.7	89.4 ± 0.79	0.302	−22.3
7	1:4.5	1.75	0.35	149.2	84.2 ± 1.22	0.288	−23.2
8	1:6	1.75	0.20	374.7	87.9 ± 0.85	0.342	−26.4
9	1:4.5	1.75	0.35	149.3	84.1 ± 1.16	0.287	−23.2
10	1:6	1	0.35	418.9	86.5 ± 0.95	0.358	−26.8
11	1:3	1.75	0.20	132	59.8 ± 0.87	0.139	−18.4
12	1:3	2.5	0.35	121.8	66.9 ± 1.26	0.099	−18.2
13	1:4.5	1	0.20	219	72.2 ± 0.85	0.298	−25.6
14	1:3	1	0.35	141.6	62.4 ± 0.78	0.157	−23.5
15	1:6	1.75	0.5	365.8	92.1 ± 0.92	0.321	−25.9

at pH-7.4; this finding lead the development of a UV–Visible spectrophotometer approach to estimating THC and the method was validated according to guidelines of International conference on harmonization (Sharma et al., 2021). Since THC is a hydrophobic substance, in-vitro experiments were performed using tween 80 (at a concentration of 0.5%) and simulated intestinal fluid (pH-7.4) to increase THC solubility and attain the sink condition. The developed procedure was verified in accordance with ICH standards. A diffusion approach using a dialysis membrane was used for in vitro drug release investigations (Rahman et al., 2019). Dialysis membranes (molecular weight cut off: 12–14 kDa) were presoaked in distilled water for 12 h before the in-vitro tests, and then 10 mg of THC and optimized THC-SLN equivalent to 10 mg of THC was injected into each end and tied off. Dialysis tubes containing THC and SLN were stored in conical flasks with simulated intestinal fluid (pH 7.4 + 0.5% tween 80). The samples were agitated in an incubator bath shaker at 100 rpm and 37 ± 1 °C. A 1 ml sample of the dissolving media was taken at a set interval and then analyzed using a UV–visible spectrophotometer. We were able to keep the sink in working order by constantly replenishing the withdrawn volume with new dissolving media.

2.8.4. Drug release kinetics

The optimal formulation release kinetics were calculated using various mathematical models, including the zero-order, first order, Korsmeyer-Peppas, and Higuchi models. The in vitro drug release data is shown as a function of time as a zero-order model. It demonstrated prolonged drug release without tablet disintegration (Wojcik-Pastuszka et al., 2019). To produce a straight line, first-order kinetics must be observed as the cumulative log percentage of the drug still present over time (Dash et al., 2010). The mathematical expression of the mechanism of sustained-action medication, including drug release from the matrix system, was achieved in the Higuchi model. According to the Fickian diffusion theory, the drug's release rate is proportional to the square root of the amount of time that passes. To visualize the data, we take the square root of the time (Bruschi, 2015) and plot it against the cumulative percentage of drug release. Release kinetics by the Korsmeyer-Peppas model (Chen et al., 2020) is used for the first 60% of cumulative drug release, taking into account both non-fickian and fickian diffusion behavior and the value of the coefficient. To calculate the release kinetics of medication using the Korsmeyer-Peppas model (Dash et al., 2010), a plot of the cumulative percentage of drugs released over time in log format is obtained.

2.8.5. Morphological study via TEM

Morphological studies of optimized formulation were conducted using a transmission electron microscope (TEM, Hitachi - H-7500, Japan). The optimized SLN formulation was diluted and stained using 1% w/v phosphotungstic acid (a negative stain) and then observed under TEM for morphological investigation.

2.8.6. DSC study

Before DSC (differential scanning calorimeter) analysis, the water content of the SLN was removed by lyophilization. Thermograms of the drug, lipid, and their physical mixture were obtained using DSC Q20 V24.11 Build 124. PerkinElmer- DSC-8000 was utilized to obtain the DSC thermogram of lyophilized optimized SLN. The dried samples of optimized SLN (5–10 mg) were put in an aluminum pan and scanned with a heating rate of 10 °C/minute in a 50–300 °C temperature range against the reference standard (Yasir et al., 2017).

2.8.7. FTIR study

Spectrum 400 FT-IR/FIR Spectrometer, Perkin Elmer, USA was used for FTIR Study of THC, GMS, their physical mixture, and the lyophilized optimized THC-SLN using KBr pellet system. The absorption bands with characteristic peaks were obtained in the range of 4000–650 cm^{-1}.

2.9. In vivo studies

Albino Wistar rats (175 ± 25 g) collected from the animal House of PBRI, Bhopal were used to conduct animal studies. Experiments were conducted after prior approval by Institutional Animal Ethics Committee (IAEC), under Reference No. – PBRI/IAEC/08–22/027 from PBRI, Bhopal.

2.9.1. Pharmacokinetic study

Albino Wistar rats were acclimatized for seven days before the experiment in standard in-house conditions. Rats were kept on free water access for 14–16 h before the experiment and pharmacokinetic study of the THC and optimized THC-SLN. In two groups of rats (n = 3), suspension of THC in tween 80 (group I) and optimized THC-SLN (group II) were taken for pharmacokinetic studies. The group I rats were administered orally with the suspension of THC by gavage 80 mg/kg at a single dose and rats of group II were administered with the amount of optimized THC-SLN equivalent to 80 mg/kg. A blood sample was collected from the caudal vein at at 0, 0.5, 1, 3, 6, 12, and 24 h intervals by nicking each rat's tail and kept in heparinized micro-centrifuge tubes. To compensate for

the blood loss, normal saline (0.3 ml) was administered to rats after each serial sampling. Plasma was obtained by centrifuging the heparinized blood at 10000 rpm for 10 min. Plasma was stored at −80 °C before HPLC analysis (Shukla et al., 2017; Zhang et al., 2018). The pharmacokinetic parameters of THC and THC-SLNs were calculated and compared to check the significance of results using an unpaired *t*-test. The significance level was checked based on $p < 0.05$ and all data are presented as mean ± SD.

2.9.1.1. HPLC analysis. The method developed by D'Souza *et al.* was slightly modified and used to conduct HPLC analysis (D'Souza and Devarajan, 2013). HPLC analysis was performed using an RP-HPLC instrument equipped with a PDA detector (SPD-M20A, Shimadzu, Japan), an auto-sampler, Phenomenex, C_{18} (4.6 × 250 mm i.d., 5 μm particle size), and an LC-solution software.

The mobile phase used was the mixture of Solvent A (Acetonitrile) Solvent B (Methanol) and solvent C (Water) (40:23:37v/v). The column temperature of 25℃, the flow rate of 1.0 ml/min, and the isocratic elution mode was used with 50 μL injection volume. Detection was carried out at 280 nm.

The chromatogram of the blank was obtained by injecting the precipitating plasma using acetonitrile, filtered through membrane filters (0.22 μ Millipore). For the chromatogram of standard THC, the stock solution of THC (1 mg/mL) was prepared in acetonitrile. The predetermined concentrations of stock solution were diluted with acetonitrile to obtain the working solutions. Each working solution in 10 μL concentration was spiked separately in 90 μL of plasma to obtain the calibration sample solutions. The clear supernatant obtained after ultracentrifugation of prepared solutions at 15000 rpm, for 15 min at 4 °C was filtered through membrane filters (0.22 μ Millipore), and injected in the HPLC system in 50 μL volume (Prisilla et al., 2012).

500 μL of acetonitrile was added to the stored pharmacokinetic study samples and vortexed for 1 min. The clear supernatant obtained after ultracentrifugation of the mixture at 15000 rpm, for 15 min at 4 °C was filtered through membrane filters (0.22 μ Millipore) and injected in the HPLC system in 50 μL volume.

2.9.2. Pharmacodynamic study

2.9.2.1. Animals. Albino Wistar rats were procured from the Animal House of PBRI, Bhopal were housed at 22 ± 2 °C in four groups in separate cages having six animals each. Animals were given a standard diet (water ad libitum and golden feed, New Delhi) and kept at light: dark cycle (12:12) (El-Far et al., 2017).

2.9.2.2. Induction of diabetes. Rats were injected with STZ intraperitoneally (i.p.) at a single dose of 60 mg/kg body weight for the induction of diabetes. STZ dose was prepared by dissolving it in ice-cold 0.1 M citrate buffer. STZ-induced hypoglycemia was overcome by giving glucose solution (5%) to all the rats overnight. Animals were considered as diabetic with blood glucose levels above 200 mg/dl on the 3rd day of STZ injection (Li et al., 2009, Zafar et al., 2021). After the 4th day of the STZ injection, treatment with THC and optimized THC-SLN was started, which was considered as the 1st day of treatment, and treatment was continued up to 28 days. During treatment, blood glucose level and body weight were observed at 0, 7, 14, 21, and 28 days (Anchi et al., 2019).

2.9.2.3. Experimentation. Four groups of rats (n = 6) were used. Except for Group I, diabetes was induced in all the groups by the above-mentioned procedure. On the 1st day of treatment, animals of Group I were considered as normal control and given blank SLN (5 ml/kg) only. The animals of Group II were considered as diabetic control, and given blank SLN (5 ml/kg), group III animals received the pure THC suspension (dose, 80 mg/kg) (Pari and Murugan, 2005), and group IV animals received optimized THC-SLN (80 mg/kg) per day. All doses were given p.o. up to 28 days.

2.9.2.4. Statistical analysis. One-way ANOVA followed by the Bonferroni test was used. The value $p < 0.05$ was considered significant. All the data were presented as mean ± SD.

2.10. Stability studies

The optimized formulation was stored at temperature/relative humidity conditions 25 ± 2℃/60%±5% and 40℃±2℃/75%±5% for 180 days and its particle size, % entrapment efficiency, and PDI was checked at specific time intervals (Agarwal et al., 2020).

3. Results and discussion

3.1. Preliminary screening

3.1.1. Selection of lipid

The maximum solubility of THC was obtained in the glyceryl monostearate (7%) followed by the compritol 888 ATO (4%), cetostearyl alcohol (3%), stearic acid (1%), palmitic acid (1%), and dynasan114 (0.5%).

3.1.2. Selection of surfactant and co-surfactant

SLNs were prepared using Tween 80 and soy lecithin as a surfactant and co-surfactant respectively.

3.1.3. Selection of drug, lipid, and surfactant concentration

Acceptable results were obtained using the drug-to-lipid ratio of 1:6 with 2.5 % surfactant (Tween 80) and 0.5 % co-surfactant (soy lecithin).

3.2. Statistical analysis

The 3-D response surface and 2-D counter plots depict the response surface analysis of factors and responses as shown in Figs. 1 and 2. The quadratic model was suggested by the sequential model sum of squares which is based on the highest-order polynomial for all the responses. ANOVA was used for statistical analysis of data obtained for all the responses given in Table 3.

3.2.1. Analysis of particle size

The particle size was obtained in the range of 121.8–418.9 nm. The model F-value of 568.53, p-value < 0.05 suggested that model was significant. In the case of particle size (Y_1), A, B, C, AB, BC, A^2, B^2, and C^2 were significant model terms with p-values<0.05. The model was improved by removing all the insignificant terms. The predicted R^2 was in close agreement with the adjusted R^2. The Adeq precision indicated by the signal-to-noise ratio of Y_1 was found to be 67.5452, which is greater than 4, suggesting the fitness of the selected model. The lack of fitness was observed as non significant. In the present study, *The positive sign of A^2 depicted that particle size was increased with an increase in the drug to lipid ratio.* While the negative coefficient obtained for factors B and C shows the reduction in particle size with an increased surfactant and co-surfactant concentration. A positive value of B^2 and C^2 indicated an increase in surfactant concentration beyond the limit could exceed the particle size. The interaction between GMS and tween 80(AB) could decrease the particle size as depicted in **Equation (3)**.

$$Y_1 = +149.27 + 119.54A - 33.16B - 6.90C - 20.35AB + 7.58BC + 92.39A^2 + 8.34B^2 + 7.82C \quad (3)$$

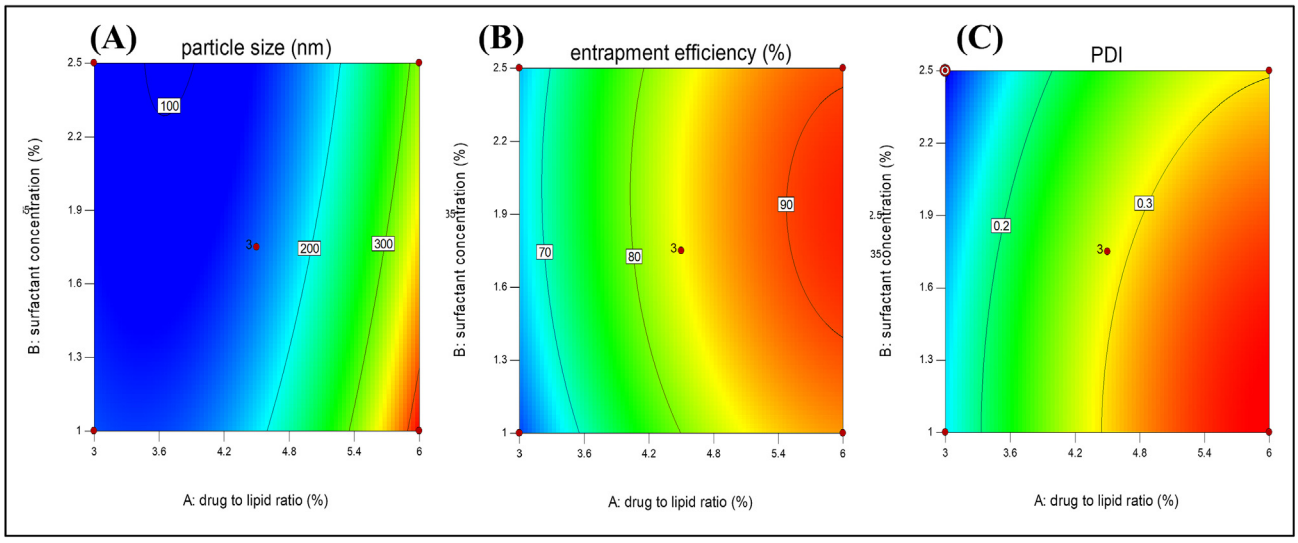

Fig. 1. 2-D response surface plots of selected responses (A) particle size, (B) % EE and (C) PDI.

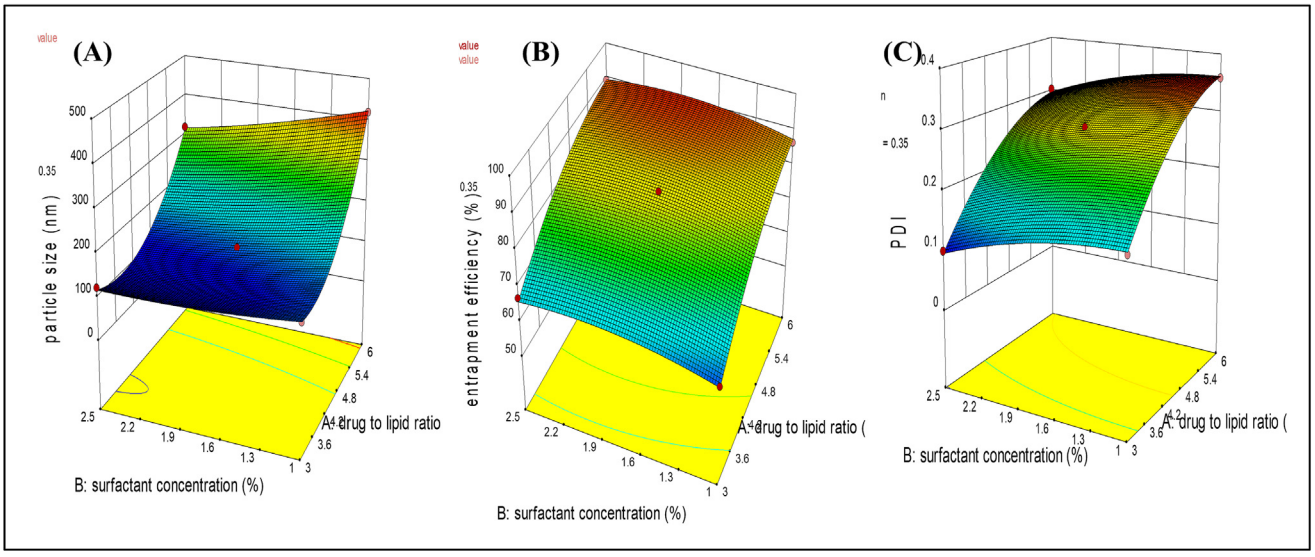

Fig. 2. 3-D response surface plots of selected responses (a) particle size, (b) % EE and (c) PDI.

Table 3
Statistical analysis using ANOVA.

Parameters	Particle size	Percent Entrapment efficiency	PDI
p-value	2.67	1.23	1.96
F-value	0.99	0.99	0.99
Adjusted R^2	0.99	0.99	0.99
Predicted R^2	0.98	0.95	0.98
Adeq Precision	67.54	40.26	66.47

3.2.2. Analysis of percent entrapment efficiency

The percent entrapment efficiency was observed in the range of 59.8 ± 0.878−−−92.1 ± 0.925%. The model F-value of 174.16 and p-values < 0.05 imply the model was significant with A, B, C, AC, BC, A^2, B^2, and C^2 significant model terms. The insignificant lack of fit proved the variability of responses by model. The predicted R^2 and adjusted R^2 difference was<0.2 which indicated a reasonable agreement between them. The signal-to-noise ratio was 40.268; indicating an adequate signal as the value was greater than 4. Hence, this model can be used for navigation of the design space. The response surface plots and equation for entrapment efficiency are depicting all the three-factor contributing to increasing the entrapment efficiency. The positive sign of factor A indicated the higher the drug-to-lipid ratio will result in maximum entrapment efficiency. The positive symboled factors B and C in the equation showed that the surfactant and co-surfactant concentration also increase the entrapment efficiency. While the negative coefficient of AC and BC showed that soy lecithin tends to decrease the effect of tween 80 and lipid on entrapment efficiency by altering their functions as shown in **Equation (4)**. While more than sufficient concentration of any of the variables will decrease the entrapment efficiency as explained by the negative coefficient of A^2, $B^{2,}$ and C^2 this could be the effect of gel formation, micelles, etc. The maximum drug entrapment was achieved with 1:6 (a drug-to-lipid ratio) with 1.75 % of a surfactant and 0.5 % of the co-surfactant.

$$Y_2 = +84.13 + 12.21A + 1.49B + 3.75C - 1.28AC - 2.42BC - 5.24A^2 - 2.59B^2 - 1.67C^2 \quad (4)$$

3.2.3. Analysis of PDI

The model with an F-value of 452.97 and p-values<0.05 was found to be significant. In PDI, significant model terms were A, B, C, BC, A^2, B^2, and C^2. The equation was generated by improving the model using all the significant model terms only. The lack of fitness was marginally non significant. The Predicted R^2 was found within close agreement with the adjusted R^2. An adequate signal was indicated by a signal-to-noise ratio of 66.474. The response surface plot and equation depict an increase in PDI with the drug-to-lipid ratio and a decrease by an increase in the surfactant and co-surfactant concentration (Alhalmi et al., 2022b). The negative coefficient of AC and BC showed that the soy lecithin together with surfactant and lipid tend to decrease the PDI and make the homogeneous dispersion. The negative coefficient of A^2, B^2, and C^2 indicated the decrease in PDI with the excess amount of lipid, surfactant, and co-surfactant, as shown in **Equation (5)**.

$$Y_3 = +0.2873 + 0.1004A - 0.0323B - 0.0094C - 0.0065BC - 0.0425A^2 - 0.0158B^2 - 0.0130C^2 \quad (5)$$

3.3. Selection of optimized formulation

To obtain the small particle size, optimum PDI, and higher entrapment efficiency, the optimization was done using a design expert. The predicted value for all three independent variables is shown in the overlay plot. The drug-to-lipid ratio, concentration of surfactant, and co-surfactant (1:4.16, 1.21, and 0.4775%) were used to prepare the optimized batch based on the desirability index as shown in Fig. 3. The predicted values of responses i.e., 147.337 nm for particle size, 82.371% for entrapment efficiency, and 0.2647 for PDI were obtained. The observed values for particle size, entrapment efficiency, and PDI of the optimized batch were found to be 147.1 nm, 83.58 ± 0.838 %, and 0.265 respectively, and these were found very close to predicted values. The optimized batch was characterized using FTIR, DSC, morphological studies, in-vitro drug release, drug release kinetics, and stability studies.

3.4. Characterization of optimized THC-loaded SLN

3.4.1. Particle size, zeta potential, and PDI

An optimized batch was observed with a particle size of 147.1 nm and PDI of 0.265 as shown in Fig. 4. The zeta potential of optimized THC-loaded SLN was −24.6 mV, representing the stability of the formulation as shown in Fig. 5.

3.4.2. Drug content

The optimized formulation's drug content was found to be 99.5 ± 0.45%.

3.4.3. In vitro release study

The plain drug suspension showed 85.50 % release in 24 h. While the optimized formulation showed a burst release of 27 % in the first 2 h followed by a sustained release of 71.04% up to 24 h as shown in Fig. 6.

3.4.4. Drug release kinetics

The correlation coefficient (R^2 = 0.9883) was found with the highest value for the Korsmeyer-peppas model as shown in Fig. 7. The value of diffusion exponent N was found between 0.45 and 0.89.

3.4.5. Morphological study via TEM

The particles were found to be spherical in size, monodispersed on the surface, and showed no clumps in the morphological studies of optimized formulation (Fig. 8**)**. The particles were in close agreement with the size obtained using a zetasizer.

3.4.6. DSC studies

Fig. 9 shows the DSC thermograms of THC, glyceryl monostearate, physical mixture, and optimized formulation. In the DSC thermogram of THC and GMS, a sharp endothermic peak at 96.59℃ with an enthalpy energy of 362.2 J/g and at 59.97℃ with an enthalpy energy of 353.0 J/g were observed respectively. Only a slight shift of peaks from 59.97℃ to 57.19℃ (GMS) and from

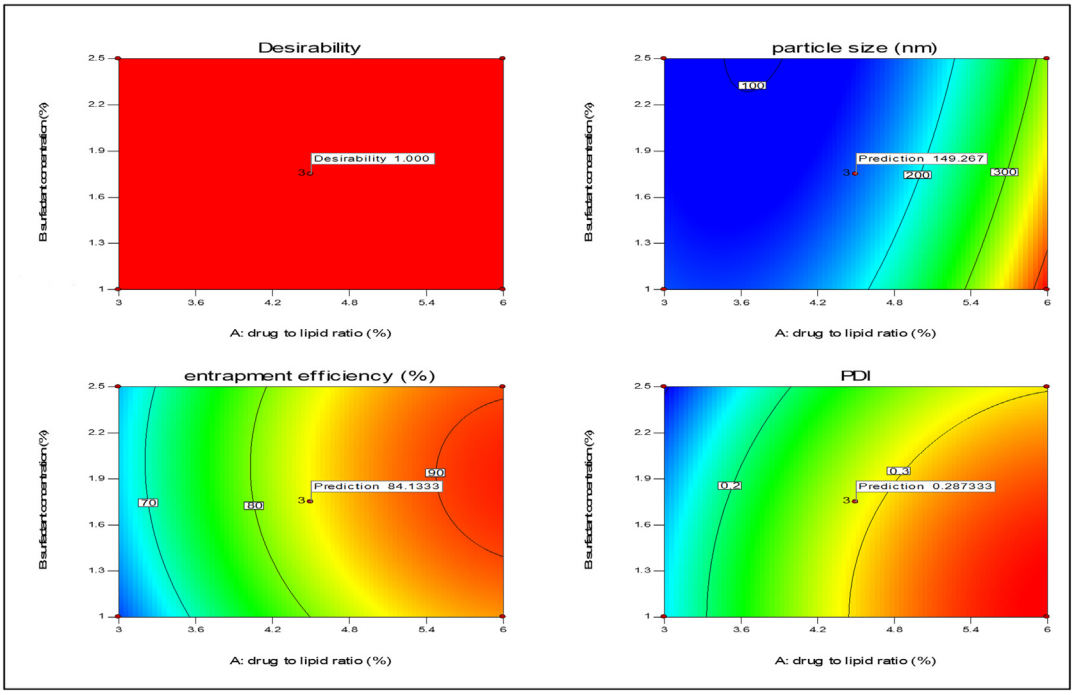

Fig. 3. Desirability index for selection of optimum formulation.

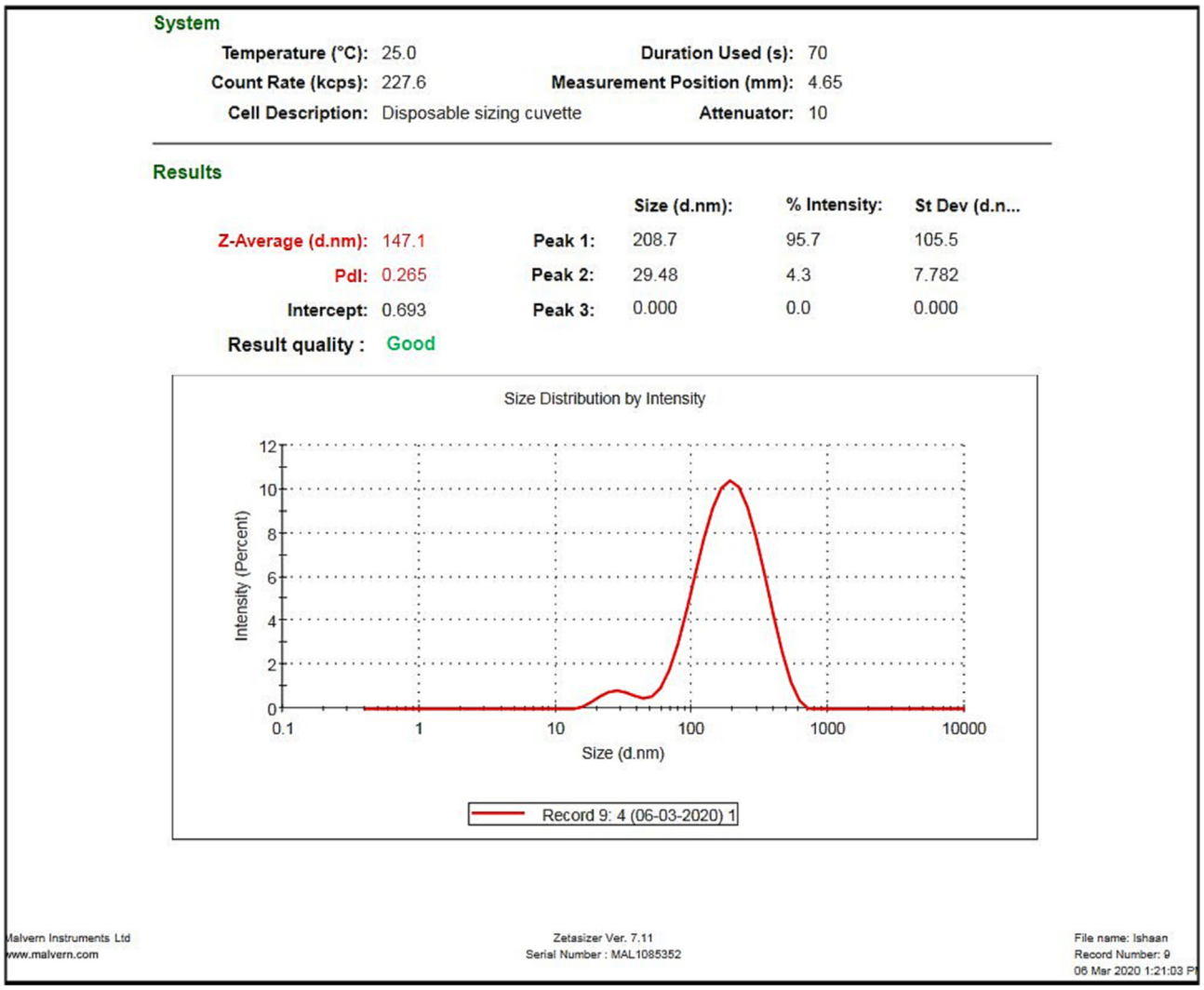

Fig. 4. The particle size of optimized SLN.

96.59℃ to 87.86℃ (THC) from the physical mixture was observed. The peak of THC disappeared in the optimized formulation and the peak of GMS was broadened and shifted from 59.97℃ to 54.95℃ in formulation.

3.4.7. FTIR studies

All the characteristic peaks were present in the physical mixture with slight shifting (Fig. 10). The comparison of the characteristic peaks of functional groups in the interpretation of THC, physical mixture, and optimized formulation is shown in Table 4. In optimized THC-SLN, the presence of peaks for all the groups was confirmed only there was a foremost change in the characteristics peak of -C-OCH_3 stretching in the optimized formulation, but it was still within the specified range of the IR chart.

3.5. In vivo studies

3.5.1. Pharmacokinetic study

The comparison between the AUC of the plain THC suspension and optimized THC-SLN is shown in Fig. 11.

The pharmacokinetics parameters such as C_{max}, T_{max}, $AUC_{(0\text{-}t)}$, $AUC_{(0\text{-}inf)}$, K_{el}, $T_{1/2}$, V_d, Cl, and relative bioavailability (F) were obtained using plasma concentration versus time profile and results are shown in Table 5. The half-life of optimized THC-SLN (14.46 ± 3.33 hrs) was significantly higher than a plain drug suspension (6.1 ± 1.8 hrs). The elimination rate constant, clearance, and V_d of the optimized THC-SLN were lower than plain THC suspension. C_{max} and $AUC_{(0\text{-}inf)}$ were found to be 6.56 and 10.92 folds higher than the plain drug suspension. The optimized THC-SLN showed relative bioavailability of 1092%.

3.5.2. Pharmacodynamic studies

3.5.2.1. Effect of optimized THC-SLN on diabetes mellitus. The blood samples were taken at different days intervals and mean blood glucose levels were analyzed for all the groups; as shown in Table 6. Diabetes was induced in animals significantly ($p < 0.001$) by using STZ. Fasting blood glucose level was observed at greater than 200 mg/dl compared to non-diabetic control. Stable mean blood glucose level was observed in animals of group I throughout the study. Animals of Group II were found diabetic significantly ($p < 0.001$) by the end of the study with a mean blood glucose level of 309.4 ± 3.528 compared to non-diabetic control. Mean blood glucose level was reduced (266.0 ± 9.022–128.7 ± 8.503 mg/dl) in Group III animal (pure THC suspension), significantly ($p < 0.001$) compared to group II (diabetic control). Blood glucose level was found to be decreased by 51.6% by the end of the 28th day. A mean blood glucose level (283.2 ± 7.188–102.6 ± 7.274 m g/dl) was changed significantly ($p < 0.001$) in Group IV (STZ

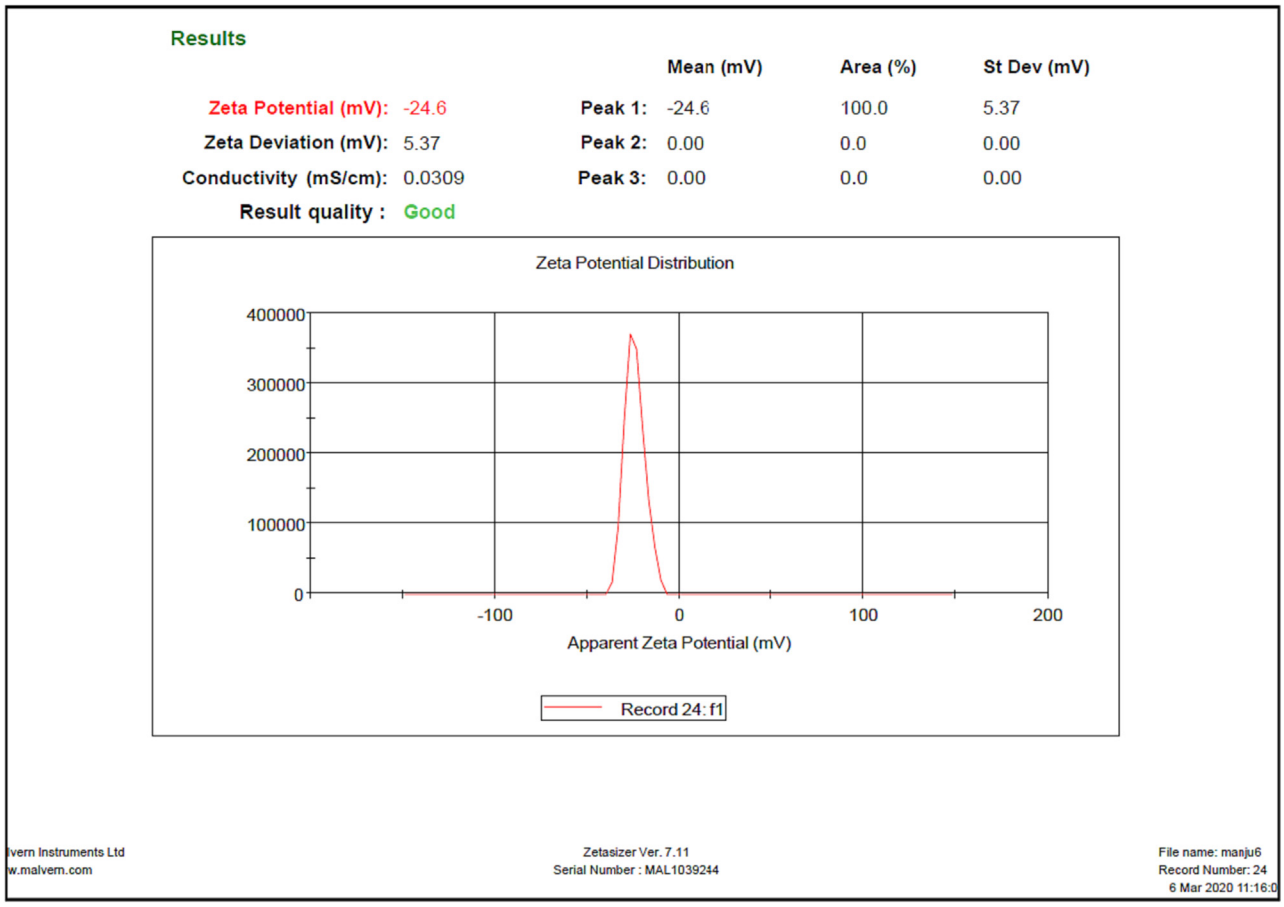

Fig. 5. Zeta potential of optimized THC-loaded SLN.

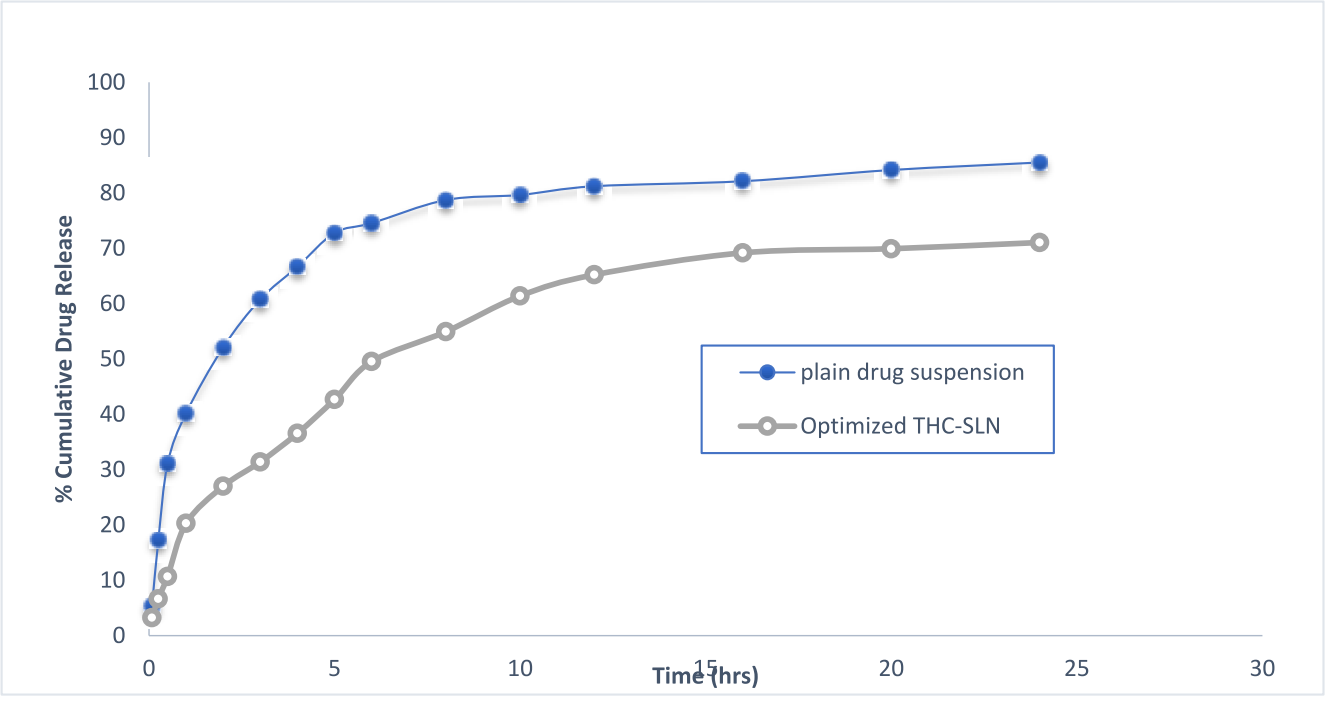

Fig. 6. In vitro release of free drug and optimized batch (n = 3).

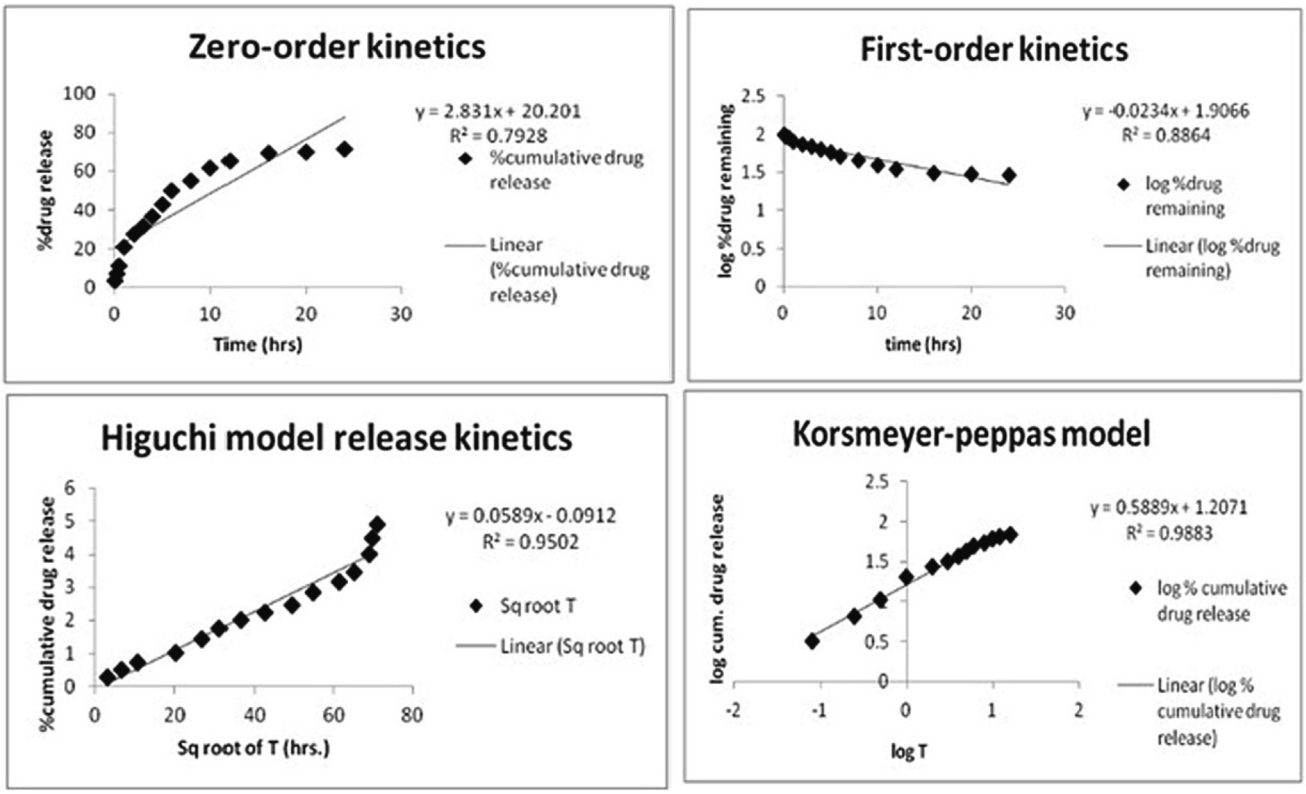

Fig. 7. Release kinetics of optimized batch.

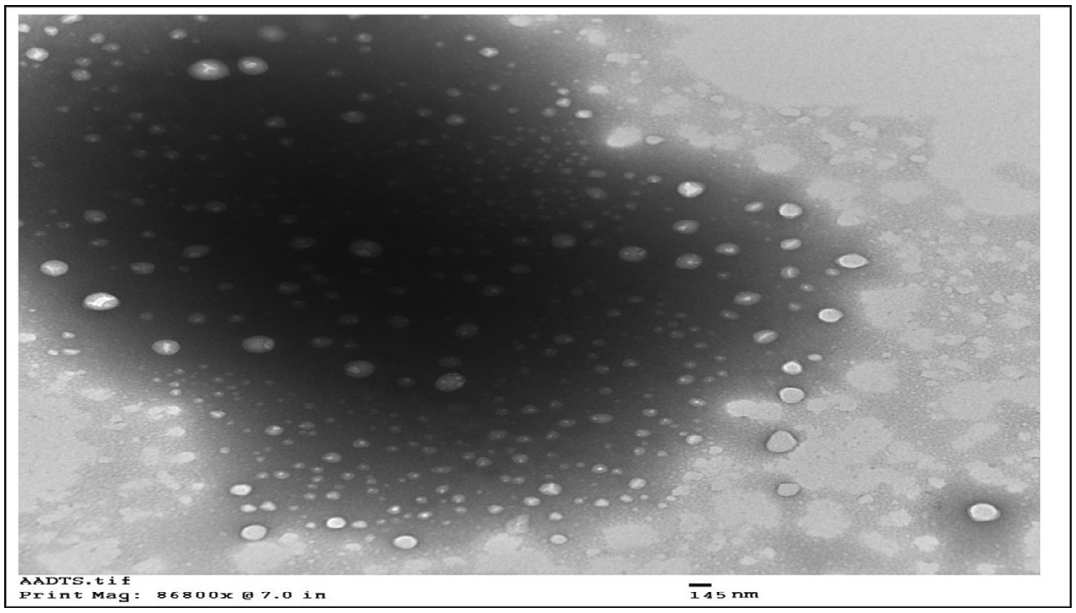

Fig. 8. TEM image of optimized THC-SLN.

(60 mg/kg) + optimized THC-SLN) compared to group III (STZ (60 mg/kg) + pure THC suspension) and group II (diabetic control) animals. Blood glucose level was found to decrease up to 63.7% by the 28th day of the study as shown in Fig. 12. Several reasons can be worked for the antidiabetic activity of THC, such as its effectiveness in reducing the blood glucose level, metabolism of carbohydrates, restoration of enzyme activity, and insulin binding to its receptors (Rivera-Mancía et al., 2015). A study showed that THC improves glucose homeostasis by reducing the blood glucose level, enhancing the secretion of insulin from existing β-cells, increasing animal body weight, and increasing plasma insulin level by reducing gluconeogenic enzyme activity in the STZ-induced diabetic rats

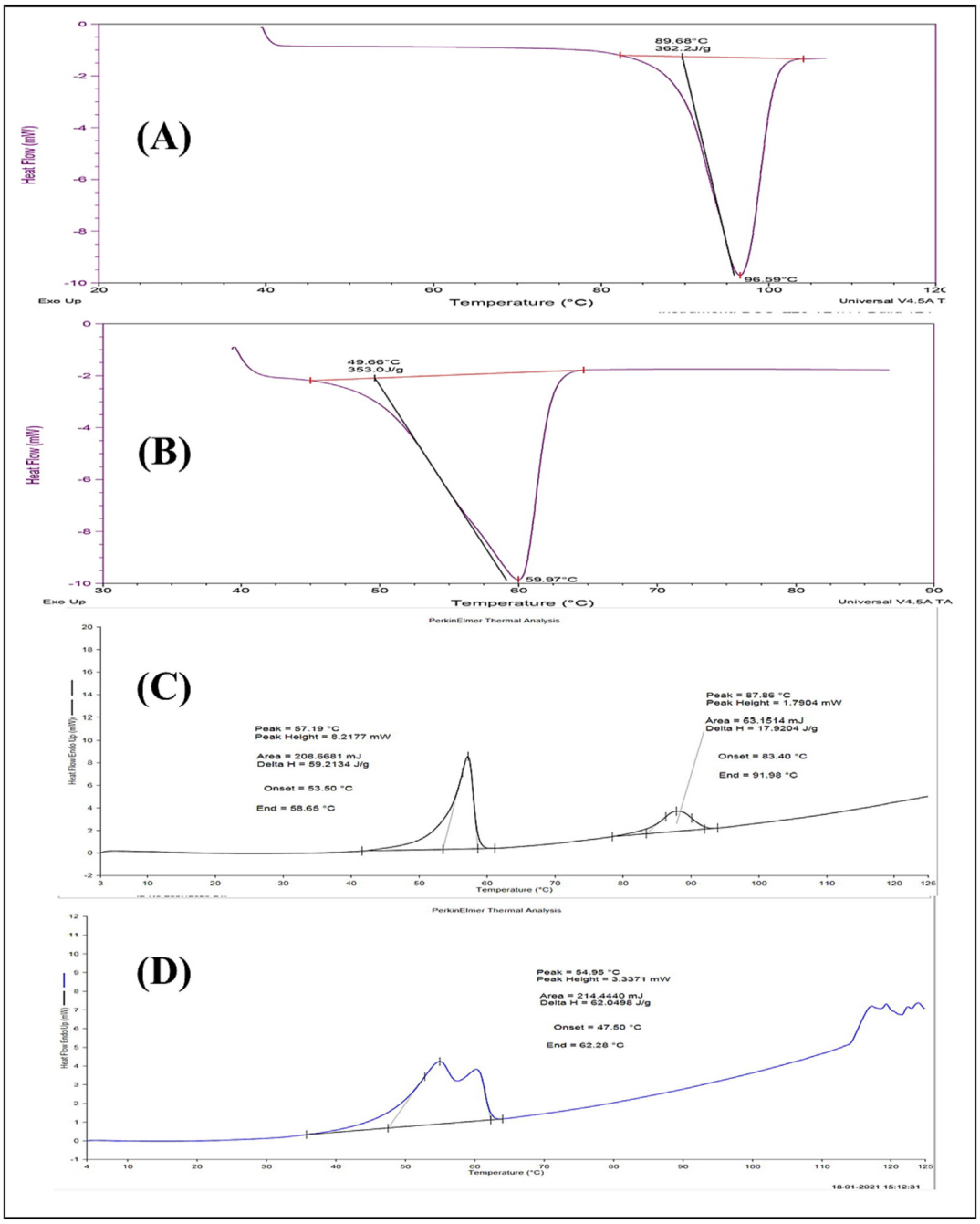

Fig. 9. DSC Thermogram of (a) THC (b) GMS (c) Physical Mixture (d) Optimized THC-SLN.

(Pari and Murugan, 2005). THC showed higher antioxidant activity as compared to curcumin due to the increased enzyme activity involved (Murugan and Pari, 2006a).

3.5.2.2. Effect of optimized THC-SLN on body weights. The body weight of non-diabetic control animals was stable throughout the study. At the same time, the body weight of group II animals was drastically decreased significantly in comparison with non-diabetic control ($p < 0.001$). The body weight of animals receiving the pure drug suspension and optimized THC-SLN improved significantly ($p < 0.001$) than diabetic control animals. A more improvement in body weight of animals receiving optimized THC-SLN was observed compared to plain drug suspension significantly ($p < 0.05$) as shown in Fig. 13.

3.6. Stability studies

A stability study was conducted for six months period as shown in Table 7. Slightly more changes were observed in the entrapment efficiency at accelerated conditions compared to room temperature, while the physical appearance of the formulation was the same.

After 6 months, the particle size of the optimized formulation was changed from 147.1 to 167.2 nm at room temperature conditions, and from 147.1 nm to 213.0 nm at accelerated conditions. In accelerated conditions, PDI was quite stable for 30 days, but it was found to be increased at the end of 180 days. While at room temperature conditions, PDI was stable for up to 6 months. Insignificant changes were observed in the particle size, entrapment

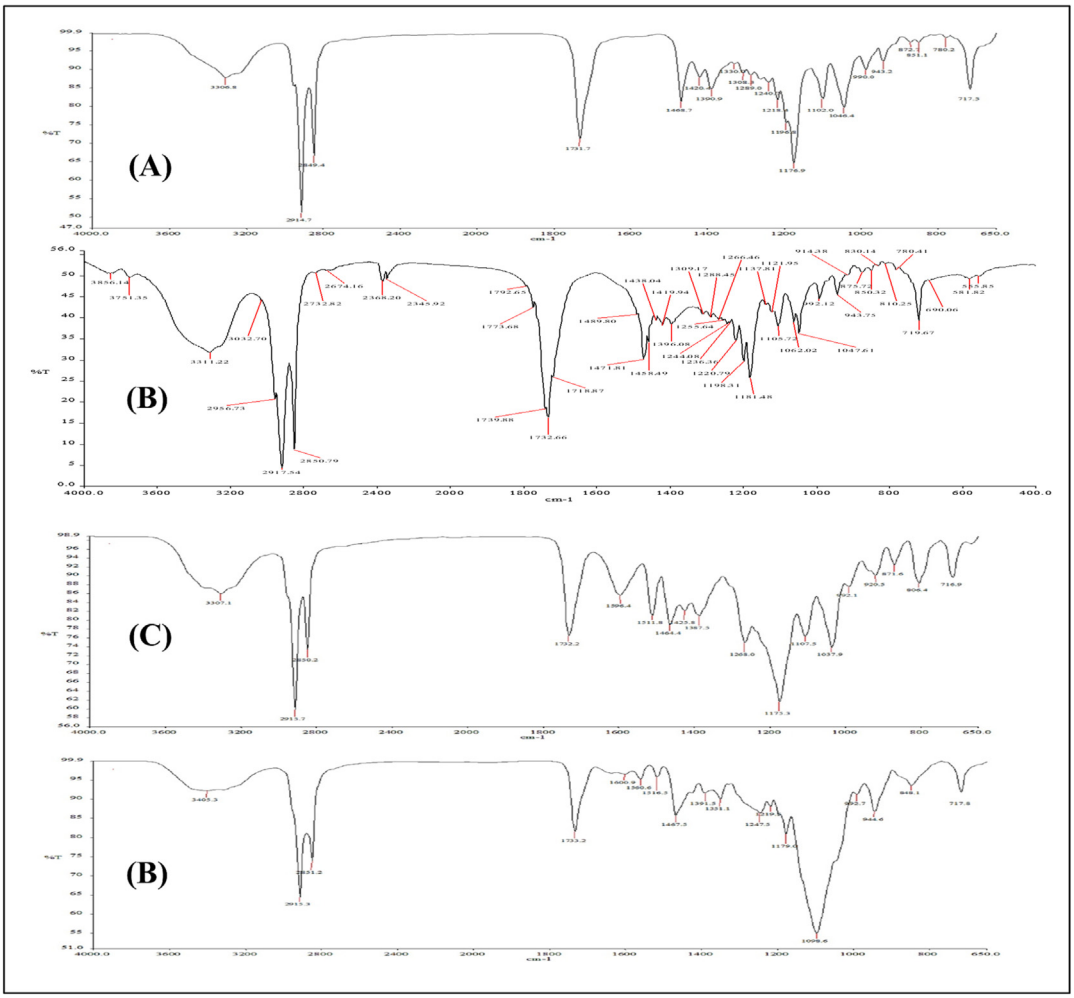

Fig. 10. FTIR spectra of (A) tetrahydrocurcumin (B) GMS (C) physical mixture (D) optimized THC-SLN.

Table 4
FTIR interpretation of tetrahydrocurcumin, physical mixture, and optimized formulation.

S. No.	Interpretation	IR absorption bands (cm^{-1}) (THC spectra)	IR absorption bands (cm^{-1}) (Physical Mixture)	IR absorption bands (cm^{-1}) (Optimized THC-SLN)
1	OH stretching of the phenol group	3306.8	3307.1	3405.3
2	C = O stretching of Carbonyl	1731.7	1732.2	1733.2
3	enol C-O stretching	1289.0	1268.0	1247.5
4	C–H bending of the methyl groups	1468.7	1464.4	1467.5
5	-C-OCH3 stretching	1046.4	1037.9	992.7
6	O–H bending	1420	1425.8	1391.5
7	C-OH	1102.0	1107.5	1098.6
8	C–H Strechings of alkane	2914.7, 2849.4	2915.7, 2850.2	2915.3, 2851.2

efficiency, and PDI. Particle size was with a narrow size distribution even after 6 months. PDI was<0.5 results showing that uniform distribution was maintained throughout the stability period.

4. Discussion

Glyceryl monostearate was selected as a lipid for SLN preparation based on results obtained by the solubility study, because maximum solubility of THC was obtained in the glyceryl monostearate, as it contains mono-, di- as well as triglycerides, so it can solubilize maximum drug amount. we have selected tween 80 as a surfactant and soy lecithin as a co-surfactant. Tween 80 helps to decrease the particle size and increase the entrapment efficiency in SLN. A study proved that pluronic F68 produced a formulation with larger particle size and PDI than compared to tween 80 and the reason may be, pluronic F68 has a higher HLB value than tween 80 (Iizhar et al., 2016). Since the drug was slightly aqueous soluble as compared to curcumin so soy lecithin would help to enhance the entrapment efficiency, also less amount of lipid will be required for the formulation of SLN by the addition of soy lecithin as a co-surfactant. Trials were conducted for the selection of drug-to-lipid ratio, surfactant, and co-surfactant concentration. As we observed that less amount of lipid was required for the preparation

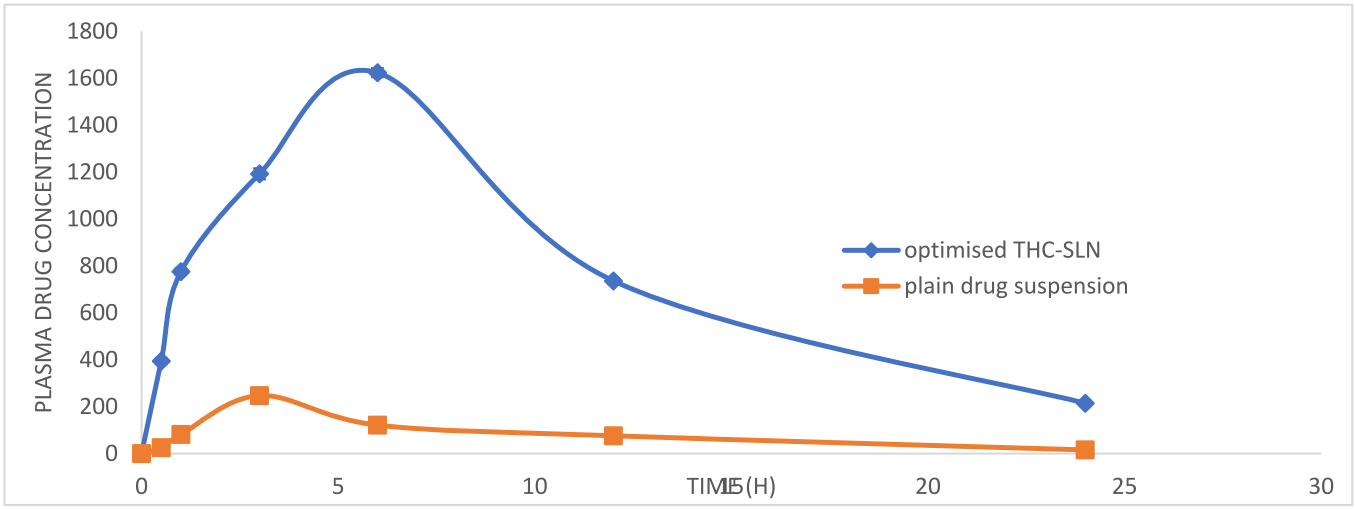

Fig. 11. Comparison of pharmacokinetics study of plain THC suspension and optimized THC-SLN (n = 3).

Table 5
Pharmacokinetics parameters of optimized THC-SLN and plain THC suspension (n = 3).

Pharmacokinetic parameter	Optimized THC-SLN*	Plain THC suspension*	Unpaired T-test, p-value
$C_{max)}$ (ng/ml)	1624.43 ± 58.35	247.35 ± 26.38	0.0007, extremely significant
$AUC_{(0-t)}$ (ng/ml*h)	19411.70 ± 421.97	2049.35 ± 271.92	<0.0001, extremely significant
$AUC_{(0-inf)}$ (ng/ml*h)	23921.80 ± 566.82	2181.88 ± 357.90	<0.0001, extremely significant
T_{max}(hrs)	6 ± 0.00	3 ± 0.00	–
$K_{el}(h^{-1})$	0.047 ± 0.037	0.113 ± 0.09	–
$_{t1/2}$(hrs)	14.46 ± 3.33	6.1 ± 1.8	0.034, significant
V_d (L)	102.16 ± 13.20	669.51 ± 27.28	0.0014, a very significant
Cl (L/h)	4.81 ± 2.58	75.72 ± 9.63	0.0065, significant
F	1092%	–	–

*The values are expressed as Mean ± S.D.

Table 6
Pharmacodynamic study showing the mean blood glucose level (mg/dl) of rats (n = 6).

S. No.	Treatment	Blood glucose level (mg/dl)				
		0 Day	7 Day	14 Day	21 Day	28 Day
1	Group I (Non-diabetic control)	104.1 ± 2.43	109.7 ± 4.44	107.1 ± 3.54	111.0 ± 4.30	109.4 ± 2.83
2	Group II (Diabetic control)	294.1 ± 3.59***	299.7 ± 4.75	304.1 ± 4.40	307.0 ± 4.41	309.4 ± 3.52***
3	Group III (THC Suspension, 80 mg/kg)	266.0 ± 9.02***	238.1 ± 6.80***	192.6 ± 9.95***	156.4 ± 8.60***	128.7 ± 8.50***
4	Group IV (THC- SLN,80 mg/kg)	283.2 ± 7.18***	219.5 ± 8.78***	173.5 ± 6.55***	129.2 ± 7.46***	102.6 ± 7.27***

of SLN, the reason for the same may be some of the portions may be solubilized in the aqueous phase (Zhang et al., 2013) and the use of soy lecithin as a co-surfactant (Tan et al., 2017). Total 15 formulations were prepared by utilizing box behnken design. The statistical analysis of experimental data for all three responses was done using ANOVA. The high level of positive significance of factor A showing the contribution of lipids in increasing the particle size, the reason may be the coalesce in the formulation and increase in viscosity observed with increased concentration of lipid. Also, the additional space provided by the lipid for the entrapment of the drug so decreases the total surface area and increases the particle size (Shah and Pathak, 2010). At a high drug-to-lipid ratio, due to viscosity sonication gets affected, and produces large particles (Iizhar et al., 2016). On the other hand, smaller particle size was obtained upon increasing the surfactant andco-surfactant concentration. As the surfactants form a stable dispersion by reducing the surface free energy and surface tension. They break down the droplets of lipid melt and prevent the formation of aggregates thus decreasing the particle size (Khames et al., 2019). But positive significant B^2 and C^2 indicated that beyond the limit, an increase in surfactant and co-surfactant concentration results in the formation of micelles and could also increase the particle size (Kumar et al., 2022b). The decrease in the particle size was observed with the interaction of lipid and sufactant that might be due to the surfactant which surrounds the lipid droplets to decrease its size while the interaction of lipid and soy lecithin tends to increase the particle size as together they tried to entrap all the drug by strengthening the film formed (Tan et al., 2017). The maximum % entrapment efficiency was obtained with high drug to lipid ratio. The reason may be the mixture of acylglycerols provides more space for the entrapment of drugs (Shah and Pathak, 2010). Surfactant and co-surfactant also increased the % entrapment efficiency up to some extent. The increasing effect was due to tween 80 (Iizhar et al., 2016) and soy lecithin (Tan et al., 2017) which increase the film strength of formulation. The polynomial equation showed that excess amount of any of the variables resulted in decrease in the

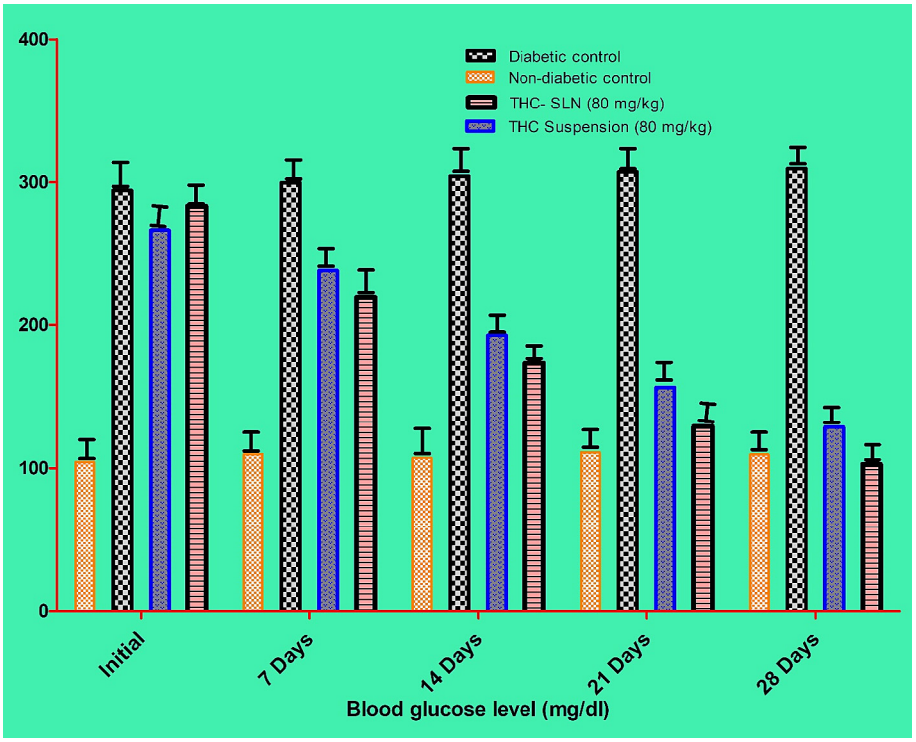

Fig. 12. Pharmacodynamic study showing the mean blood glucose level (mg/dl) at different time intervals of different groups of rats (n = 6).

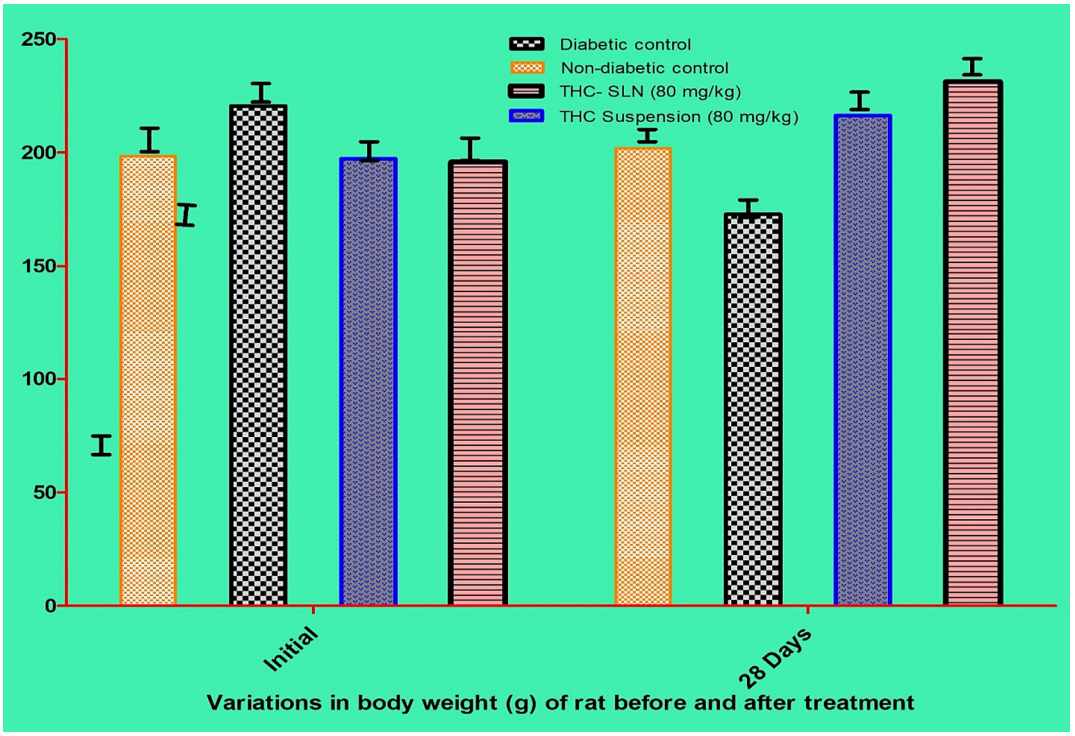

Fig. 13. Pharmacodynamic study showing the effect of formulations on the body weight (g) of treated rats (n = 6).

% entrapment efficiency. This may be due to the formation of gel and micelles, etc. The maximum drug entrapment was achieved with the higher lipid concentration with the optimum amount of surfactant and co-surfactant. The homogeneous distribution of particles in SLN could be explained by PDI near 0 and for the narrow particle size distribution acceptable PDI is up to 0.5 (Agarwal et al., 2020). In our study, PDI was found to be decreased by increasing the surfactant concentration and increased by increasing drug to lipid ratio. The reasons may be the same as with the particle size. Co-surfactant also decreased the PDI and contributed in the formation of homogeneous dispersion. Polynomial equation showed that excess amount of lipid, surfactant, and co-surfactant,

Table 7
Six months stability profile of optimized THC-SLNs (n = 3).

Duration		25C ± 2C/60% ± 5% RH				40C ± 2C/75% ± 5% RH			
S. No.	Time (Days)	Physical Appearance	EE ± SD (%)	Particle Size (nm)	PDI	Physical appearance	EE ± SD (%)	Particle Size (nm)	PDI
1	0	Off white suspension throughout the study	83.58 ± 2.13	147.1	0.265	Off-white suspension throughout the study	83.58 ± 0.83	147.1	0.265
2	30		81.09 ± 1.73	148.0	0.265		80.66 ± 1.96	149.6	0.269
3	60		80.93 ± 1.66	149.7	0.267		78.01 ± 1.48	154.3	0.278
4	90		80.08 ± 1.78	151.8	0.269		75.17 ± 1.83	176.8	0.291
5	180		78.49 ± 1.35	167.2	0.272		69.95 ± 1.76	213.0	0.316

decreased the PDI, this could be explained as no free drug will be present in suspension with the use of an excess amount of these three variables. Optimization was done using the design expert software to obtain the formulation batch with small particle size and high % entrapment efficiency. The optimized batch's results were found in very close agreement with the predicted values, which proved the significance of our design. The prediction of the stability of a formulation is done by Zeta potential, which is expressed as the difference in electrical voltage in surface-charged particles. The zeta potential within the range of +/−30 mV is considered ideal (Andrade et al., 2019). The zeta potential of all the THC-loaded SLN was observed within the range, which represents the formulations' stability. Drug content analysis confirmed that drug was not degraded during preparation of SLN. Higher solubility of THC was obtained in the alkaline medium than the acidic medium in the solubility studies conducted for the selection of disssolution media. The results were also supported by Kakkar et al. and co-workers in their studies, where THC offers superior stability at pH 7.4 (Kakkar et al., 2018). Simulated intestinal fluid (pH-7.4) along with Tween 80 (0.5%) was used as a dissolution media for in-vitro release stuides. The burst release was observed initially because there may be some drug present at the outer region of the formed SLN and later on sustained effect was observed due to the slow release of the drug from the inner core of SLN (H. Bhatt et al., 2018). In the drug release kinetics study, the highest value of the correlation coefficient (R^2 = 0.9883) was observed for the korsmeyer Peppas model. This showed the release of drugs from the matrix in a controlled manner (Sharma et al., 2021). As the value of diffusion exponent N was between 0.45 and 0.89, the drug release was following the non-fickian diffusion mechanism (Arora et al., 2011). This indicated that the mechanism of drug release was diffusion followed by erosion. Firstly the media was diffused into the matrix in a controlled manner then the outer layer of SLN was eroded or solubilized to allow drug release in dissolution media (Sermkaew et al., 2013). In the morphological study conducted using TEM, particles were found spherical in shape and mono-dispersed on the surface without showing any clumps. The DSC thermogram of the THC and GMS revealed that these are crystalline in nature. Both, THC and GMS are found compatible with each other in DSC studies of physical mixture. The disappearance of peak of THC in the optimized formulation confirmed the conversion of the drug to the amorphous from crystalline form. The peak of GMS was broadened and shifted in formulation indicating the formation of SLN (Wadetwar et al., 2020). The shifting in peak may be due to the reduction of particle size in SLN than lipid in bulk, the presence of co-surfactant and surfactant, and the provided high surface area (Gardouh, 2013; Wang et al., 2016). All the characteristic peaks were present in the FTIR of physical mixture with slight shifting, which confirmed no chemical interaction between lipid and drug (Wadetwar et al., 2020). In optimized THC-SLN FTIR spectra, the presence of peaks for all the groups confirmed the encapsulation of a stable form of THC in the lipid. There was a foremost change in the characteristics peak of -C-OCH_3 stretching in the optimized formulation, but it was still within the specified range of the IR chart. The presence of all the peaks of functional groups in the formulation showed that probe sonication did not alter the structure of lipids (Öztürk et al., 2019). While shifting and broadening of the peaks and reduction in density in the peaks from the peaks of the THC may be due to the formation of SLN which confirmed the hydrogen bond presence between THC and lipid (Sharma et al., 2021). In pharmacokinetic study, we have compared our optimized formulation with the plain drug suspension. The t_{max} and half-life of optimized THC-SLN were found to be higher when compared to the plain drug suspension. While clearance, elimination rate constant and V_d of the optimized formulation were found to be lower than the plain curcumin suspension, confirming the presence of the drug in the body for a longer period of time(Shukla et al., 2017). The prolonged and sustained release effect was shown by optimized THC-SLN as its C_{max} and $AUC_{(0\text{-}inf)}$ were found to be higher than the plain drug suspension. The enhanced bioavailability may be due to the SLN providing a higher surface area, thus enhancing the drug's solubilization. Lipids in the formulation bypass the portal circulation and prevent CYP3A-mediated drug metabolism. They alter the gastric residence time of the drug, so it helps increase their uptake by the lymphatic system (Baek and Cho, 2017). In anti-diabetic study of optimized THC-SLN, a quite acceptable decrease of 63.7 % was observed in the blood glucose level of the animals and found almost similar to mean blood glucose level of non-diabetic control animals by the 21st day of the treatment. Compared to plain drug suspension marked improvement was observed in the body weight in animals received optimized THC-SLN. Several reasons may have worked for anti-diabetic activity of THC, such as its effectiveness in reducing the blood glucose level, restoration of enzyme activity, and insulin binding to its receptors (Pari and Murugan, 2005). A study also reported that THC could improve glucose homeostasis by enhancing insulin secretion from existing β-cells, increasing the body weight of the animal and increasing plasma insulin level by reducing gluconeogenic enzyme activity in the STZ-induced diabetic rats (Pari and Murugan, 2005). THC showed higher antioxidant activity as compared to curcumin due to the increased enzyme activity involved (Murugan and Pari, 2006a). During the stability study, SLN were found with the narrow particle size distribution even after 6 months at accelerated and room temperature conditions. Slight changes were observed in the % entrapment efficiency at accelerated conditions when compared to room temperature. In contrast, no differences were observed in the physical appearance of the drug, which showed that no crystallization of the drug was occurred during storage period. The heterogenecity was observed in PDI at the end of 180 days at accelerated conditions, while it was almost stable throughout the period at room temperature. The stability study concluded that the formulation can be stored for an extended period at room temperature. Slight changes can be observed at the accelerated conditions. These findings showed that SLN could be a promising drug delivery system for controlled delivery of tetrahydrocurcumin in the management of diabetes mellitus and can be preferred over the conventional dosage forms.

5. Conclusions

Glyceryl monostearate was found to be a lipid-soluble solvent in the development of THC-SLN. The experimental batches were used to determine the ideal concentrations of surfactant and co-surfactant. To construct effective SLN formulations, a box Behnken design was used. The effects of the independent variables (a drug to lipid ratio, surfactant concentration, and co-surfactant concentration) and their interaction on the desired outcomes were investigated (particle size, entrapment efficiency, and PDI). Particle size, entrapment efficiency, and PDI were all measured to be 147.1 nm, 83.580 ± 838%, and 0.265 for the optimized batch, respectively, which was extremely near to the predicted values. The in vitro investigation found that the medication was released in a rapid burst at first, possibly because it was concentrated on the outer layer, and then gradually decreased in concentration over 24 h. The morphological analysis demonstrated that the particles were monodispersed and spherical. An enhanced formulation was reported to have much greater bioavailability and antidiabetic potential than ordinary drug dispersion. Therefore, SLN may serve as a transport mechanism for THC in the treatment of diabetes.

Funding

This research was funded by Princess Nourah bint Abdulrahman University Researchers Supporting Project number (PNURSP2023R141), Princess Nourah bint Abdulrahman University, Riyadh, Saudi Arabia. Thankful also to Researchers Supporting Project number (RSP2023R379), King Saud University, Riyadh, Saudi Arabia.

CRediT authorship contribution statement

Jai Bharti Sharma: Conceptualization, Writing – original draft, Methodology. **Shailendra Bhatt:** Conceptualization, Supervision. **Abhishek Tiwari:** Writing – review & editing, Software. **Varsha Tiwari:** Writing – review & editing. **Manish Kumar:** Writing – review & editing, Supervision. **Ravinder Verma:** Software, Formal analysis. **Deepak Kaushik:** Validation, Writing – review & editing, Writing – original draft. **Tarun Virmani:** Validation, Formal analysis. **Girish Kumar:** Writing – review & editing. **Omkulthom Al kamaly:** Funding acquisition, Writing – review & editing. **Asmaa Saleh:** Funding acquisition, Writing – review & editing. **Mohammed Khalid Parvez:** Funding acquisition, Writing – review & editing. **Abdulsalam Alhalmih:** Formal analysis.

Declaration of Competing Interest

The authors declare that they have no known competing financial interests or personal relationships that could have appeared to influence the work reported in this paper.

Acknowledgement

The authors extend their appreciation to Princess Nourah bint Abdulrahman University Researchers Supporting Project number (PNURSP2023R141), Princess Nourah bint Abdulrahman University, Riyadh, Saudi Arabia. Thankful also to Researchers Supporting Project number (RSP2023R379), King Saud University, Riyadh, Saudi Arabia. The authors acknowledge the MM College of Pharmacy, Mullana, Ambala, India for providing the necessary facilities.

Sample Availability

Samples of the synthesized nanoparticles are available from the authors.

References

Agarwal, S., Murthy, R.S.R., Harikumar, S.L., Garg, R., 2020. Quality by design approach for development and characterisation of solid lipid nanoparticles of quetiapine fumarate. Curr. Comput. Aided Drug Des. 16, 73–91. https://doi.org/10.2174/1573409915666190722122827.

Alhalmi, A., Amin, S., Beg, S., Al-Salahi, R., Mir, S.R., Kohli, K., 2022a. Formulation and optimization of naringin loaded nanostructured lipid carriers using Box-Behnken based design: In vitro and ex vivo evaluation. J. Drug Deliv. Sci. Technol. 74,. https://doi.org/10.1016/J.JDDST.2022.103590 103590.

Alhalmi, A., Beg, S., Almalki, W.H., Alghamdi, S., Kohli, K., 2022c. Recent advances in nanotechnology-based targeted therapeutics for breast cancer management. Curr. Drug Metab. 23, 587–602. https://doi.org/10.2174/1389200223666220514151110.

Alhalmi, A., Amin, S., Khan, Z., Beg, S., Al kamaly, O., Saleh, A., Kohli, K., 2022b. Nanostructured Lipid Carrier-Based Codelivery of Raloxifene and Naringin: Formulation, Optimization, In Vitro, Ex Vivo, In Vivo Assessment, and Acute Toxicity Studies. Pharmaceutics 14, 1771. https://doi.org/10.3390/pharmaceutics14091771

Anchi, P., Khurana, A., Swain, D., Samanthula, G., Godugu, C., 2019. Dramatic improvement in pharmacokinetic and pharmacodynamic effects of sustain release curcumin microparticles demonstrated in experimental type 1 diabetes model. Eur. J. Pharm. Sci. Off. J. Eur. Fed. Pharm. Sci. 130, 200–214. https://doi.org/10.1016/j.ejps.2019.02.002.

Andrade, L.N., Oliveira, D.M.L., Chaud, M.V., Alves, T.F.R., Nery, M., da Silva, C.F., Gonsalves, J.K.C., Nunes, R.S., Corrêa, C.B., Amaral, R.G., Sanchez-Lopez, E., Souto, E.B., Severino, P., 2019. Praziquantel-solid lipid nanoparticles produced by supercritical carbon dioxide extraction: Physicochemical characterization, release profile, and cytotoxicity. Molecules 24. https://doi.org/10.3390/molecules24213881.

Arora, G., Malik, K., Singh, I., Arora, S., Rana, V., 2011. Formulation and evaluation of controlled release matrix mucoadhesive tablets of domperidone using Salvia plebeian gum. J. Adv. Pharm. Technol. Res. 2, 163–169. https://doi.org/10.4103/2231-4040.85534.

Baek, J.-S., Cho, C.-W., 2017. Surface modification of solid lipid nanoparticles for oral delivery of curcumin: Improvement of bioavailability through enhanced cellular uptake, and lymphatic uptake. Eur. J. Pharm. Biopharm. Off. J. Arbeitsgemeinschaft fur Pharm. Verfahrenstechnik e.V 117, 132–140. https://doi.org/10.1016/j.ejpb.2017.04.013.

Ban, C., Jo, M., Park, Y.H., Kim, J.H., Han, J.Y., Lee, K.W., Kweon, D.-H., Choi, Y.J., 2020. Enhancing the oral bioavailability of curcumin using solid lipid nanoparticles. Food Chem. 302,. https://doi.org/10.1016/j.foodchem.2019.125328 125328.

Behbahani, E.S., Ghaedi, M., Abbaspour, M., Rostamizadeh, K., 2017. Optimization and characterization of ultrasound assisted preparation of curcumin-loaded solid lipid nanoparticles: Application of central composite design, thermal analysis and X-ray diffraction techniques. Ultrason. Sonochem. 38, 271–280. https://doi.org/10.1016/j.ultsonch.2017.03.013.

Bhatt, H., Rompicharla, S.V.K., Komanduri, N., Aashma, S., Paradkar, S., Ghosh, B., Biswas, S., 2018. Development of curcumin-loaded solid lipid nanoparticles utilizing glyceryl monostearate as single lipid using QbD approach: Characterization and evaluation of anticancer activity against human breast cancer cell line. Curr. Drug Deliv. 15, 1271–1283. https://doi.org/10.2174/1567201815666180503120113.

Bhatt, S., Sharma, J., Singh, M., Saini, V., 2018. Solid lipid nanoparticles: A promising technology for delivery of poorly water-soluble drugs. Acta Pharm. Sci. 56, 27–49. https://doi.org/10.23893/1307-2080.APS.05616.

Bruschi, M.L., 2015. Strategies to modify the drug release from pharmaceutical systems. Woodhead Publishing.

Chen, K., Chen, X., Han, X., Fu, Y., 2020. A comparison study on the release kinetics and mechanism of bovine serum albumin and nanoencapsulated albumin from hydrogel networks. Int. J. Biol. Macromol. 163, 1291–1300. https://doi.org/10.1016/j.ijbiomac.2020.07.043.

D'Souza, A.A., Devarajan, P.V., 2013. Rapid and simultaneous HPLC analysis of curcumin and its metabolite tetrahydrocurcumin from plasma and liver homogenates. J. Liq. Chromatogr. Relat. Technol. 36, 1788–1801. https://doi.org/10.1080/10826076.2012.698680.

Dash, S., Murthy, P.N., Nath, L., Chowdhury, P., 2010. Kinetic modeling on drug release from controlled drug delivery systems. Acta Pol. Pharm. 67, 217–223.

Dudhipala, N., Janga, K.Y., 2017. Lipid nanoparticles of zaleplon for improved oral delivery by Box-Behnken design: optimization, in vitro and in vivo evaluation. Drug Dev. Ind. Pharm. 43, 1205–1214. https://doi.org/10.1080/03639045.2017.1304957.

El-Bagory, I., Alruwaili, N.K., Elkomy, M.H., Ahmad, J., Afzal, M., Ahmad, N., Elmowafy, M., Alharbi, K.S., Alam, M.S., 2019. Development of novel dapagliflozin loaded solid self-nanoemulsifying oral delivery system: Physiochemical characterization and in vivo antidiabetic activity. J Drug Deliv Sci Technol. 54,. https://doi.org/10.1016/j.jddst.2019.101279 101279.

El-Far, Y.M., Zakaria, M.M., Gabr, M.M., El Gayar, A.M., Eissa, L.A., El-Sherbiny, I.M., 2017. Nanoformulated natural therapeutics for management of streptozotocin-induced diabetes: potential use of curcumin nanoformulation. Nanomedicine 12, 1689–1711. https://doi.org/10.2217/nnm-2017-0106.

Farsani, P.A., Mahjub, R., Mohammadi, M., Oliaei, S.S., Mahboobian, M.M., 2021. Development of perphenazine-loaded solid lipid nanoparticles: statistical optimization and cytotoxicity studies. Biomed. Res. Int. 2021, 6619195. https://doi.org/10.1155/2021/6619195.

Ganesan, P., Ramalingam, P., Karthivashan, G., Ko, Y.T., Choi, D.-K., 2018. Recent developments in solid lipid nanoparticle and surface-modified solid lipid nanoparticle delivery systems for oral delivery of phyto-bioactive compounds in various chronic diseases. Int. J. Nanomed. 13, 1569–1583. https://doi.org/10.2147/IJN.S155593.

Gardouh, A., 2013. Design and characterization of glyceryl monostearate solid lipid nanoparticles prepared by high shear homogenization. Br. J. Pharm. Res. 3, 326–346. https://doi.org/10.9734/bjpr/2014/2770.

Gaur, P.K., Mishra, S., Bajpai, M., Mishra, A., 2014. Enhanced Oral Bioavailability of Efavirenz by Solid Lipid Nanoparticles: *In Vitro* Drug Release and Pharmacokinetics Studies. Biomed Res. Int. 2014, 363404. https://doi.org/10.1155/2014/363404.

Hazzah, H.A., Farid, R.M., Nasra, M.M.A., Hazzah, W.A., El-Massik, M.A., Abdallah, O. Y., 2015. Gelucire-based nanoparticles for curcumin targeting to oral mucosa: Preparation, characterization, and antimicrobial activity assessment. J. Pharm. Sci. 104, 3913–3924. https://doi.org/10.1002/jps.24590.

Iizhar, S.A., Syed, I.A., Satar, R., Ansari, S.A., 2016. In vitro assessment of pharmaceutical potential of ethosomes entrapped with terbinafine hydrochloride. J. Adv. Res. 7, 453–461. https://doi.org/10.1016/j.jare.2016.03.003.

Kakkar, V., Kaur, I.P., Kaur, A.P., Saini, K., Singh, K.K., 2018. Topical delivery of tetrahydrocurcumin lipid nanoparticles effectively inhibits skin inflammation: in vitro and in vivo study. Drug Dev. Ind. Pharm. 44, 1701–1712. https://doi.org/10.1080/03639045.2018.1492607.

Khames, A., Khaleel, M.A., El-Badawy, M.F., El-Nezhawy, A.O.H., 2019. Natamycin solid lipid nanoparticles - sustained ocular delivery system of higher corneal penetration against deep fungal keratitis: preparation and optimization. Int. J. Nanomed. 14, 2515–2531. https://doi.org/10.2147/IJN.S190502.

Kumar, G., Virmani, T., Pathak, K., Alhalmi, A., 2022a. A Revolutionary Blueprint for Mitigation of Hypertension via Nanoemulsion. BioMed Res. Int. 2022, ID 4109874.

Kumar, G., Virmani, T., Pathak, K., Kamaly, O.A., Saleh, A., 2022b. Central composite design implemented azilsartan medoxomil loaded nanoemulsion to improve its aqueous solubility and intestinal permeability. In vitro and ex vivo evaluation. Pharmaceuticals 15. https://doi.org/10.3390/ph15111343.

Kumar, G., Virmani, T., Sharma, A., Pathak, K., 2023. Codelivery of phytochemicals with conventional anticancer drugs in form of nanocarriers. Pharmaceutics 15. https://doi.org/10.3390/pharmaceutics15030889.

Lai, C.-S., Ho, C.-T., Pan, M.-H., 2020. The cancer chemopreventive and therapeutic potential of tetrahydrocurcumin. Biomolecules 10. https://doi.org/10.3390/biom10060831.

Li, J., Jiang, Y., Wen, J., Fan, G., Wu, Y., Zhang, C., 2009. A rapid and simple HPLC method for the determination of curcumin in rat plasma: assay development, validation and application to a pharmacokinetic study of curcumin liposome. Biomed. Chromatogr. 23, 1201–1207. https://doi.org/10.1002/bmc.1244.

Murugan, P., Pari, L., 2006a. Antioxidant effect of tetrahydrocurcumin in streptozotocin–nicotinamide induced diabetic rats. Life Sci. 79, 1720–1728. https://doi.org/10.1016/j.lfs.2006.06.001.

Murugan, P., Pari, L., 2006b. Effect of tetrahydrocurcumin on plasma antioxidants in streptozotocin-nicotinamide experimental diabetes. J. Basic Clin. Physiol. Pharmacol. 17, 231–244. https://doi.org/10.1515/jbcpp.2006.17.4.231.

Murugan, P., Pari, L., 2006c. Effect of tetrahydrocurcumin on lipid peroxidation and lipids in streptozotocin-nicotinamide-induced diabetic rats. Basic Clin. Paharmacol. Toxicol. 99, 122–127. https://doi.org/10.1111/j.1742-7843.2006.pto_447.x.

Murugan, P., Pari, L., 2007. Influence of tetrahydrocurcumin on hepatic and renal functional markers and protein levels in experimental type 2 diabetic rats. Basic Clin. Paharmacol. Toxicol. 101, 241–245. https://doi.org/10.1111/j.1742-7843.2007.00109.x.

Öztürk, A.A., Banderas, L.M., Otero, M.D.C., Yenilmez, E., Şenel, B., Yazan, Y., 2019. Dexketoprofen trometamol-loaded poly-lactic-co-glycolic acid (PLGA) nanoparticles: Preparation, in vitro characterization and cyctotoxity. Trop. J. Pharm. Res. 18, 1–11. https://doi.org/10.4314/tjpr.v18i1.1.

Padhye, S.G., Nagarsenker, M.S., 2013. Simvastatin solid lipid nanoparticles for oral delivery: formulation development and in vivo evaluation. Indian J. Pharm. Sci. 75, 591–598.

Pari, L., Murugan, P., 2005. Effect of tetrahydrocurcumin on blood glucose, plasma insulin and hepatic key enzymes in streptozotocin induced diabetic rats. J. Basic Clin. Physiol. Pharmacol. 16, 257–274. https://doi.org/10.1515/jbcpp.2005.16.4.257.

Pari, L., Murugan, P., 2007. Antihyperlipidemic effect of curcumin and tetrahydrocurcumin in experimental type 2 diabetic rats. Ren. Fail. 29, 881–889. https://doi.org/10.1080/08860220701540326.

Prisilla, D.H., Balamurugan, R., Shah, H.R., 2012. Antidiabetic activity of methanol extract of Acorus calamus in STZ induced diabetic rats. Asian Pac. J. Trop. Biomed. 2, S941–S946. https://doi.org/10.1016/S2221-1691(12)60341-4.

Priyanka, K., Sahu, P.L., Singh, S., 2018. Optimization of processing parameters for the development of Ficus religiosa L. extract loaded solid lipid nanoparticles using central composite design and evaluation of antidiabetic efficacy. J. Drug Deliv. Sci. Technol. 43, 94–102. https://doi.org/10.1016/j.jddst.2017.08.006.

Rahman, M.A., Harwansh, R.K., Iqbal, Z., 2019. Systematic development of sertraline loaded solid lipid nanoparticle (SLN) by emulsification-ultrasonication method and pharmacokinetic study in sprague-dawley rats. Pharm. Nanotechnol. 7, 162–176. https://doi.org/10.2174/2211738507666190327145628.

Rana, S.S., Bhatt, S., Kumar, M., Malik, A., Sharma, J.B., Arora, D., Saini, V.K., 2020. Design and optimization of itraconazole loaded SLN for intranasal administration using central composite design. Nanosci. Nanotechnol.-Asia 10, 884–891.

Rivera-Mancía, S., Lozada-García, M.C., Pedraza-Chaverri, J., 2015. Experimental evidence for curcumin and its analogs for management of diabetes mellitus and its associated complications. Eur. J. Pharmacol. 756, 30–37. https://doi.org/10.1016/j.ejphar.2015.02.045.

Rramaswamy, R., Mani, G., Venkatachalam, S., Venkata Yasam, R., Rajendran, J.C.B., Hyun Tae, J., 2018. Preparation and characterization of tetrahydrocurcumin-loaded cellulose acetate phthalate/polyethylene glycol electrospun nanofibers. AAPS PharmSciTech 19, 3000–3008. https://doi.org/10.1208/s12249-018-1122-0.

Sermkaew, N., Wiwattanawongsa, K., Ketjinda, W., Wiwattanapatapee, R., 2013. Development, characterization and permeability assessment based on caco-2 monolayers of self-microemulsifying floating tablets of tetrahydrocurcumin. AAPS PharmSciTech 14, 321–331. https://doi.org/10.1208/s12249-012-9912-2.

Setthacheewakul, S., Kedjinda, W., Maneenuan, D., Wiwattanapatapee, R., 2011. Controlled release of oral tetrahydrocurcumin from a novel self-emulsifying floating drug delivery system (SEFDDS). AAPS PharmSciTech 12, 152–164. https://doi.org/10.1208/s12249-010-9568-8.

Shah, M., Pathak, K., 2010. Development and statistical optimization of solid lipid nanoparticles of simvastatin by using 2(3) full-factorial design. AAPS PharmSciTech 11, 489–496. https://doi.org/10.1208/s12249-010-9414-z.

Sharma, J.B., Bhatt, S., Saini, V., Kumar, M., 2021. Pharmacokinetics and pharmacodynamics of curcumin-loaded solid lipid nanoparticles in the management of streptozotocin-induced diabetes mellitus: Application of central composite design. Assay Drug Dev. Technol. 19, 262–279. https://doi.org/10.1089/adt.2021.017.

Sharma, J.B., Bhatt, S., Saini, V., Kumar, M., 2021. Development and validation of uv-visible spectrophotometric method for the estimation of curcumin and tetrahydrocurcumin in simulated intestinal fluid. Res J Pharm Technol. 14 (6), 2971–2975. https://doi.org/10.52711/0974-360X.2021.00520.

Shaveta, S., Singh, J., Afzal, M., Kaur, R., Imam, S.S., Alruwaili, N.K., Alharbi, K.S., Alotaibi, N.H., Alshammari, M.S., Kazmi, I., Yasir, M., 2020. Development of solid lipid nanoparticle as carrier of pioglitazone for amplification of oral efficacy: formulation design optimization, in-vitro characterization and in-vivo biological evaluation. J. Drug Deliv. Sci. Technol. 57,. https://doi.org/10.1016/j.jddst.2020.101674 101674.

Shukla, M., Jaiswal, S., Sharma, A., Srivastava, P.K., Arya, A., Dwivedi, A.K., Lal, J., 2017. A combination of complexation and self-nanoemulsifying drug delivery system for enhancing oral bioavailability and anticancer efficacy of curcumin. Drug Dev. Ind. Pharm. 43, 847–861. https://doi.org/10.1080/03639045.2016.1239732.

Syed, I.A., Patro, C., Alshanberi, A.M., Ansari, S.A., 2021. Statistical Designing and Characterization of Valsartan Oral Disintegrating Tablet. Adv. Pharmacol. Pharm. 9, 33–44. https://doi.org/10.13189/app.2021.090301.

Sznitowska, M., Wolska, E., Baranska, H., Cal, K., Pietkiewicz, J., 2017. The effect of a lipid composition and a surfactant on the characteristics of the solid lipid microspheres and nanospheres (SLM and SLN). Eur. J. Pharm. Biopharm. Off. J. Arbeitsgemeinschaft fur Pharm. Verfahrenstechnik e.V 110, 24–30. https://doi.org/10.1016/j.ejpb.2016.10.023.

Tan, M.-E., He, C.-H., Jiang, W., Zeng, C., Yu, N., Huang, W., Gao, Z.-G., Xing, J.-G., 2017. Development of solid lipid nanoparticles containing total flavonoid extract from Dracocephalum moldavica L. and their therapeutic effect against myocardial ischemia-reperfusion injury in rats. Int. J. Nanomed. 12, 3253–3265. https://doi.org/10.2147/IJN.S131893.

Trivedi, M.K., Panda, P., Sethi, K.K., Gangwar, M., Mondal, S.C., Jana, S., 2020. Solid and liquid state characterization of tetrahydrocurcumin using XRPD, FT-IR, DSC, TGA, LC-MS, GC-MS, and NMR and its biological activities. J. Pharm. Anal. 10, 334–345. https://doi.org/10.1016/j.jpha.2020.02.005.

Virmani, T., Kumar, G., Virmani, R., Sharma, A., Pathak, K., 2022. Nanocarrier-based approaches to combat chronic obstructive pulmonary disease. Nanomedicine 17, 1833–1854. https://doi.org/10.2217/nnm-2021-0403.

Wadetwar, R.N., Agrawal, A.R., Kanojiya, P.S., 2020. In situ gel containing Bimatoprost solid lipid nanoparticles for ocular delivery: In-vitro and ex-vivo evaluation. J. Drug Deliv. Sci. Technol. 56,. https://doi.org/10.1016/j.jddst.2020.101575 101575.

Wang, T., Ma, X., Lei, Y., Luo, Y., 2016. Solid lipid nanoparticles coated with cross-linked polymeric double layer for oral delivery of curcumin. Colloids Surf. B Biointerfaces 148, 1–11. https://doi.org/10.1016/j.colsurfb.2016.08.047.

Wojcik-Pastuszka, D., Krzak, J., Macikowski, B., Berkowski, R., Osiński, B., Musiał, W., 2019. Evaluation of the Release Kinetics of a Pharmacologically Active Substance from Model Intra-Articular Implants Replacing the Cruciate Ligaments of the Knee. Mater. (Basel, Switzerland) 12. https://doi.org/10.3390/ma12081202.

Yasir, M., Chauhan, I., Zafar, A., Verma, M., Noorulla, K.M., Tura, A.J., Alruwaili, N.K., Haji, M.J., Puri, D., Gobena, W.G., Dalecha, D.D., 2021. Buspirone loaded solid lipid nanoparticles for amplification of nose to brain efficacy: Formulation development, optimization by Box-Behnken design, in-vitro characterization

and in-vivo biological evaluation. J. Drug Deliv. Sci. Technol. 61,. https://doi.org/10.1016/j.jddst.2020.102164 102164.

Yasir, M., Sara, U.V.S., Chauhan, I., Gaur, P.K., Singh, A.P., Puri, D. and Ameeduzzafar, 2018. Solid lipid nanoparticles for nose to brain delivery of donepezil: Formulation, optimization by Box–Behnken design, in vitro and in vivo evaluation. Artif cells nanomed biotechnol. 46(8), 1838-1851. https://doi.org/10.1080/21691401.2017.1394872

Yuan, T., Yin, Z., Yan, Z., Hao, Q., Zeng, J., Li, L., Zhao, J., 2020. Tetrahydrocurcumin ameliorates diabetes profiles of db/db mice by altering the composition of gut microbiota and up-regulating the expression of GLP-1 in the pancreas. Fitoterapia 146,. https://doi.org/10.1016/j.fitote.2020.104665 104665.

Zafar, A., Alruwaili, N.K., Imam, S.S., Alotaibi, N.H., Alharbi, K.S., Afzal, M., Ali, R., Alshehri, S., Alzarea, S.I., Elmowafy, M., Alhakamy, N.A., 2021. Bioactive Apigenin loaded oral nano bilosomes: Formulation optimization to preclinical assessment. Saudi Pharm. J. 29 (3), 269–279. https://doi.org/10.1016/j.jsps.2021.02.003.

Zhang, D.-W., Fu, M., Gao, S.-H., Liu, J.-L., 2013. Curcumin and diabetes: a systematic review. Evid. Based Complement. Alternat. Med. 2013,. https://doi.org/10.1155/2013/636053 636053.

Zhang, Q., Polyakov, N.E., Chistyachenko, Y.S., Khvostov, M.V., Frolova, T.S., Tolstikova, T.G., Dushkin, A.V., Su, W., 2018. Preparation of curcumin self-micelle solid dispersion with enhanced bioavailability and cytotoxic activity by mechanochemistry. Drug Deliv. 25, 198–209. https://doi.org/10.1080/10717544.2017.1422298.